The Southern Ocean supergyre: a unifying dynamical framework identified by machine learning

Maike Sonnewald (maikes@princeton.edu)
Princeton University
Krissy Reeve
https://orcid.org/0000-0001-5615-8040
Redouane Lguensat

Article

Keywords:

Posted Date: January 27th, 2023

DOI: https://doi.org/10.21203/rs.3.rs-2448588/v1

Additional Declarations: There is **NO** Competing Interest.

Version of Record: A version of this preprint was published at Communications Earth & Environment on May 5th, 2023. See the published version at https://doi.org/10.1038/s43247-023-00793-7.

The Southern Ocean supergyre: a unifying dynamical framework identified by machine learning

Maike Sonnewald[1,2,3], Krissy Anne Reeve[4+] and Redouane Lguensat[5+]

1: Princeton University, Princeton, New Jersey, USA
2: University of Washington, Seattle, Washington, USA
3: NOAA/Geophysical Fluid Dynamics Laboratory, Princeton, New Jersey, USA
4: Alfred-Wegener-Institut Helmholtz-Zentrum for Polar and Marine Research, Department of Physical Oceanography, Bremerhaven, Germany
5: Institut Pierre-Simon Laplace, IRD, Sorbonne Université, Paris, France
+: these authors contributed equally to this work

The Southern Ocean closes the global overturning circulation and is key to the regulation of carbon and heat, biological production, and sea level. However, the dynamics of the general circulation and upwelling pathways remain poorly understood. Here, a unifying framework is proposed invoking a semi-circumpolar 'supergyre' south of the Antarctic circumpolar current: a massive series of 'leaking' sub-gyres spanning the Weddell and Ross seas that are connected and maintained via rough topography that acts as scaffolding. The

supergyre framework challenges the conventional view of having separate circulation structures in the Weddell and Ross seas and suggests a limited utility for climate applications of idealized models and conventional zonal averaged frameworks. Machine learning was used to reveal areas of coherent driving forces within a vorticity-based analysis. Predictions from the supergyre framework are supported by available observations and could aid observational and modelling efforts of the climatically key region undergoing rapid change.

Introduction

The ocean is a central component of the climate system, for example, storing over 90% of the anthropogenically introduced heat from 1971 to 2010 [1]. The large-scale circulation is key to such storage, transporting waters meridionally (north-south). The Southern Ocean, encircling the Antarctic continent is a key component of the component of the global scale meridional circulation: warm surface waters are made dense and sink at high northern latitudes, and the global loop is closed via upwelling which largely happens in the Southern Ocean. The heat release by upwelled waters along the coast of Antarctica impacts important processes, such as, melt rates of land based ice which is a key tipping point in the Earth system associated with drastic impacts on sea level [2, 3]. Despite its climatically key role, many open questions remain regarding how the circulation in the Southern Ocean is realised and maintained, and substantial model bias persists [4]. Even large-scale currents such as the Antarctic Circumpolar Current (ACC) and the upwelling key to modulating climate remain poorly understood, and the relatively few observational estimates exist of sufficient length and time scales. Focusing on the large-scale dynamics of the Southern Ocean leading to upwelling, the present work elucidates key driving features that could aid both model development and observational strategies. captured, and the present highlights key driving forces that could focus development.

The Southern Ocean subpolar gyres, regions of large-scale resirculation, are instrumental in the upwelling of warm waters, and thus in the modulation of the overturning circulation [5–7]. Gyre circulation is implicated in bringing warmer waters associated with the ACC towards the Antarctic coast where dense waters are formed. Despite the key role of gyre circulation, many open questions remain about how it is realised an supported, and in turn our ability to predict how the Southern Ocean and overturning overall will change in a warmer world is unclear. Conventionally, gyre circulation in the Southern Ocean is discussed referring to two separate entities: the Weddell and Ross gyre systems [8] in the Atlantic and Pacific sectors respectively (Fig. 1a). However, open questions remain about even basic features specific to the gyre circulation, such as, what determines the Eastern end of the gyre, and what role topography plays in maintaining the circulation. This has serious implications for monitoring strategies and understanding the spatial heterogeneity of observed changes [9–11].

Two obstacles remain central to understanding gyre circulation in the Southern Ocean. First, the observational data from the south of the ACC and approaching the Antarctic continent are limited both in temporal and spatial coverage. The problem of lacking data is discussed further below. Second, existing numerical modelling and theoretical work seeking to understand fundamental dynamics have been restricted to idealised efforts that do not capture realistic subpolar gyres. The theoretical framework preferentially used leans heavily on a zonally averaged two-dimensional rendition of the Southern Ocean circulation, understanding the overturning as a residual between the wind driving steepening of isopycnals (lines of equal density), and the opposing eddy-circulation that acts to flatten isopycnals [12]. While useful, the two-dimensional view neglects a number of potentially key features of the observed circulation, including the impact of zonal asymmetries and large-scale gyre circulation. Gyre circulation could be described as a standing meander or a very large eddies, but the dynamics that give rise to gyre circulation is complex, advecting tracers over large distances and impact the meridional stratification in a zonally inhomogeneous manner [13, 14], rather than just locally flatten isopycnals. While the impact of gyre circulation on the ACC has been studies in [15] and in [5] looking at ridge geometry, only [7] moved closer to a 'realistic' geometry adding a zonal ridge. All these works rely on idealised and simplified channel models. The two-dimensional exploration of the circulation persists despite the evident zonal heterogeneity in warming seen over recent decades [9–11]. Elucidating the dynamical drivers in a realistic framework is the focus of the present work, where a vorticity based exploration guided by machine learning is used to explore the driving forces of the circulation through a gyre-circulation focused lens.

One reason why a simplified theoretical framework has prevailed when investigating the Southern Ocean circulation is the overwhelming complexity of the circulation patterns in the region. Recently, machine learning methods are being used to fuel progress within prediction, numerical modeling and beyond, speeding up and refining existing tasks (see review in [16, 17]). Here, the novel machine learning framework from Sonnewald *et al.* (2019) is used *forge new knowledge*, specifically also avoiding a 'black box' approach.

Here, a new semi-circumpolar supergyre framework is proposed, emerging south of the ACC from a combination of several dynamical regimes, as a continuously connected series of 'sub-gyres' that encompass the circulation in the Weddell and Ross Sea in a 'leaky' recirculation. The supergyre framework is proposed as a unifying framework for understanding and monitoring Southern Ocean upwelling, as a semi-circumpolar structure. It could be used to elucidate the composition and complex pathways of the Circumpolar Deep Waters (CDW) that are upwelled within the gyre circulation. Limited existing observations show support for the proposed framework by confirming a series of sub-gyres, including in the Indian Ocean sector of the Southern Ocean [13, 14, 18–23]. Guided by clustering based machine learning, this insight could refine model representations and guide observational strategies. In addition, this work illustrated how machine learning can be used to gain new knowledge and lead to advances in theoretical understanding, complementing insight gained from conventional idealised approaches. The remainder of the introduction is structured as follows: first we introduce the barotropic vorticity framework which provides the core foundation of our approach, before discussing the importance of defining gyre boundaries. We then introduce the Southern Ocean circulation and the meridional overturning circulation before lastly introducing the concept of machine learning.

Understanding wind gyre circulation using a barotropic vorticity framework

While the circulation in the Southern Ocean is often investigated using a two-dimensional, zonally averaged framework, we here use a framework that lends itself to investigating gyre circulation and revealing the source of zonal asymmetries: the barotropic vorticity framework. Note that the data used is from a full complexity realistic ocean state estimate (described below). Wind gyres are classically understood using a friction-framework in a subtropical Northern Hemisphere context. A classical wind gyre is seen as an area of clockwise circulation that emerges from a balance between a negative wind stress curl and advection by positive planetary vorticity, bounded by continents on either side. In the Southern Ocean, features, such as, the continental boundaries are lacking. Here, two aspects of gyre circulation in the Southern Ocean are discussed in a realistic model setup. First, the spatial role of topography in the absence of continental scale boundaries. Second, the lack of a concrete eastern boundary and its implications for the zonal extent of the circulation and resultant impact on the location of upwelling. Overall, the present paper suggests that a framework centered on the spatial extent of the initiation of gyre-like circulation as given by topography can lead to skillful predictions. The unifying theory was arrived at using machine learning based objective regime discovery that can highlight where coherent physical drivers are acting [24, 25]. While the regimes in Sonnewald et al. (2019) are global, the focus here is on the dynamical regimes present in the Southern Ocean (Fig. 1).

Describing how meridional flows develop, early works [26–28] recast the intractably complicated full equations by taking the curl of the depth-integrated momentum equations, arriving at the barotropic vorticity (BV) equation (See Supplementary A for a summary of Sonnewald et al., 2019). The steady BV balance under incompressibility is expressed as:

$$\beta V = \nabla \times (p_b \nabla H) + \nabla \times \tau + \nabla \times \mathbf{A} + \nabla \times \mathbf{B}, \tag{1}$$

where $\beta = \partial f / \partial y$ is the northward derivative of the Coriolis parameter (f), $V = \int \rho v \mathrm{d}z$ is the depth-integrated northward mass transport from density ρ and meridional velocity v, ∇ is the horizontal gradient operator, p_b is the pressure at the bottom, $H = h + \eta$ is the bottom depth. H is the water column thickness, where h is the distance from the resting ocean surface to the bottom topography and η the sea surface height (SSH) anomaly. The external stress produced by wind and bottom friction is denoted τ, and $\mathbf{A}$ and $\mathbf{B}$ the depth integrals of the nonlinear and the horizontal viscous terms, respectively [29].

There is a long history of using the BV equation to describe gyre circulation that has been extended to the Southern Ocean [30]. In early seminal work using flat-bottom domains [26–28], a description of gyre circulation as friction dominated emerged. Later works began to stress the impact of bathymetry [31, 32]. Recent work emphasizes the balance between the wind stress and the bottom pressure torques (BPT) as potential key drivers of meridional transport and gyre circulation [29, 33–35]. The first term on the right hand side of Eq. 1 is the bottom pressure torques ($\nabla \times (p_b \nabla H)$), which represents the direct effect of topography on the flow through ∇H. The bottom pressure torques is important for flow crossing f/H contours, as seen both in observations [36] and identified using unsupervised machine learning on numerical model output [24]. Next, the usefulness of machine learning is demonstrated for investigating the various roles of the terms in the BV equation in the Southern Ocean.

The importance of determining the gyre boundaries

A central inference from studying the wind gyres in the subtropical Northern Hemisphere is that gyre formation requires a sink of vorticity that is, for example, found in the continental boundaries. In the BV equations, the non-linear terms provide a sink of vorticity. Areas where the vorticity input by the wind is negative and locally balanced by the positive advective component are referred to as in 'Sverdrup balance' [26, 37], which is synonymous with wind gyres and meridional flow (subtropical North Atlantic example in Supplementary B). The strength of the gyre is set by the wind stress curl, rather than the absolute magnitude [38–41].

How the boundaries of the gyre are defined and determined impact conclusions of how driving forces interact, as also stressed by Stewart *et al.*, (2021). The presence of continents forming longitudinal barriers in the subtropical Northern Hemisphere represents the overall constraint, and this can be expressed by assessing where geostrophic contours (f/H) are blocked. Conservation of potential vorticity results in flow being aligned with the geostrophic contours. In the subtropical North Atlantic, this results in a well-defined Gulf Stream in the west, along with a well defined but weaker return flow to the east marking the eastern edge. Without such blocked geostrophic contours, the flow would be largely zonal to conserve potential vorticity. For gyre circulation to arise, a sink of vorticity must be present that nominally is recognised as being given by closed geostrophic contours.

Understanding how the flow is realized within the constraint of conserving potential vorticity is very sensitive to the area chosen for study. Defining the areal extent of a gyre therefore plays an important role in making general statements about the role of driving forces. As first expressed by Holland (1972) using an idealized numerical model, baroclinic flow over variable-depth topography establishes a dominant area-integrated barotropic vorticity balance between the wind stress curl and the bottom pressure torque. This topographically-dominated gyre regime is in contrast to the frictionally-dominated gyre regime [27, 38]. Here, this point is made to highlight the importance of the area considered when making conjectures. More recently, [29] integrated latitudinally over 3° bands, and found that the wind stress approximately balanced the topographic form stress in the zonal momentum balance, which is effectively the bottom pressure torque. However, [35] noted that a bottom frictional term was needed for the formation of recirculating flows that cross the mean potential vorticity gradient along the western boundary. Overall, a key insight gained through this vein of research is an intuition that the bottom pressure torque should integrate to zero following isobaths [29, 35, 42]. [43] illustrates that the bottom pressure torque balances the wind stress curl for a specifically selected barotropic streamfunction contour. In contrast, [42] discusses how it is not intuitive that integrating around streamlines in a gyre should yield a dominant balance between wind stress curl and bottom pressure torque, and what combination is required to transition from frictionally-dominated gyre regimes to topographically-dominated gyre regimes. Overall, needing to hand-select a barotropic streamfunction contour specifically to achieve a balance between the bottom pressure torque and the wind stress curl may not be the most practical definition of a wind gyre and may skew the interpretation of associated dynamics that allow the circulation to emerge. More widely in literature, assessing properties and governing dynamics of how the driving forces balance, definitions can vary greatly ranging from simple boxes to barotropic streamlines [36, 43, 44]. For practical and climate-relevant purposes, the notion of how the areas of distinct drivers are recognized becomes very interesting in terms of understanding the dynamical balances in the Southern Ocean, through their impact on the global overturning and Earth's climate.

Studying and determining gyre boundaries is also done using purely hydrographic and lagrangian approaches. Re-evaluating the concept of gyres in the subtropics of the Southern Hemisphere led to determining the presence of a supergyre in the subtropics [45–47]. In the subtropical Southern Hemisphere, the term supergyre is used to refer to the interconnected nature of the gyres found in the subtropics of the Indian, Pacific and Atlantic basins, that are connected through 'leakages' in the Tasman and Agulhas regions. The 'leakage' between basins is possible due to the lack of land masses blocking the throughflow, and the impact of this circulation implies that changes in the supergyre in the subtropics can impact the AMOC through changing the watermass properties of its upper limb [45]. The subpolar gyre circulation in the Southern Hemisphere is the topic of the present paper, and we retain the terminology of [45–47]. However, while there is considerable leakage between the individual circulation structures in the Southern Ocean, the dynamical drivers are role in the overturning circulation are likely quite different between the subtropical and subpolar supergyres.

To summarise, it is neither practical nor objective to, for example, hand-select a barotropic streamfunction contour specifically to achieve a balance between the bottom pressure torque and the wind stress curl. Beyond not being very practical, more subjective approaches to defining a wind gyre and may skew the interpretation of associated dynamics that allow the circulation to emerge. Here, objective regime discovery is used to draw boundaries between dominant driving forces as dictated directly by areas of unique balances between drivers, rather than inferred, for example, from barotropic streamlines. Described in Sonnewald *et al.* (2019) and Supplementary A, the regions and boundaries are set by determining statistically significant areas within the co-variance space given by the terms in the BV equation, not taking geographical location into account. Supplementary B presents an example for building intuition in the conventional setting of the subtropical North Atlantic. By using the dynamical regime approach, we identify the dominating driving forces and their associated spatial distribution, and how these different areas interact.

Gyre circulation in the context of the Southern Ocean

The distinguishing feature of gyre circulation in the Southern Ocean is that there are no continental boundaries to the East and West. The BV framework is, however, still useful through the transfer of momentum via topographic interactions [30]. Thus, to explain the gyre dynamics in the Southern Ocean, where no continents act to block geostrophic contours, the ACC interactions with bathymetry are invoked as a central feature. Definitions of the ACC and its fronts vary [48], but it is seen as a highly energetic feature with an estimated total volume transport of 173.3 ± 10.7 Sv (1 Sv ≡ $10^6 m^3 s^1$, Donohue et al., 2016). Here, the ACC is defined as a circulation feature with strong Eastwards currents and areas of marked increases in the nonlinear dissipation of BV where it impacts bathymetric obstacles. The ACC is steered by bathymetry with a pressure gradient across bathymetric features ([6], among others, Fig. 3). Sea surface height is elevated downstream of topographic obstacles within the ACC, inducing lateral alongstream pressure gradients. The buildup of pressure forces the flow northward to conserve potential vorticity. This process is referred to as 'topographic steering', and through generating form stress, it generates a sink of vorticity (Fig. 3). The question posed here, is how to understand the different components of the resultant gyre-like flow to the south of the ACC and its impact on the overturning. To summarise, the vorticity sink arising from the ACC interacting with topographic obstacles can be understood as a 'dynamic western boundary' [30]. The vorticity sink that describes wind gyres in general, in the case of the Southern Ocean, is split into localised regions as a result of rough topography, which is spread zonally across the Southern Ocean, and should therefore be considered as a complex single entity.

An important distinction between the gyre circulation in the subtropical Northern Hemisphere and that in the Southern Ocean is the eastern gyre boundary, particularly in the subpolar region. In the subtropical Northern Hemisphere, the eastern edge of the gyre is resolved through a well-defined boundary current. In the Southern Ocean, no such continuous eastern current is apparent either in observations or noted in model studies to the authors' knowledge. In practical terms, the extent, strength and location of a gyre is determined using barotropic stream lines [5, 49], geopotential height anomalies or sea level [8, 50, 51]. Alternatively expert knowledge is invoked or used to supplement interpretation for its extent [8, 52, 53]. Since results of any regional model are highly sensitive to chosen boundaries, the lack of a distinct eastern boundary is problematic.

In the Southern Ocean, the two gyres commonly discussed in literature are in the Weddell and the Ross Sea, bounded by the ACC to the North [8]. Seen as separate entities, the dynamics that govern the circulation in thr Weddell and Ross seas are assumed to be very different [7]. The area between the Ross and Weddell Sea was seen as having a weak and sluggish westwards flow, until snapshots provided by hydrographic exploration, notably the World Ocean Circulation Hydrographic Program, revealed a much more complex circulation structure [22, 23, 54, 55]. The circulation in the Weddell Sea is the best studied in the Southern Ocean, reviewed in [56]. As described by [57], the Eastern boundary of the gyre-like circulation in Weddell Sea lacks a defined feature in topography and circulation, but is nominally set to 30°E, 70°E or further Eastwards [55, 58, 59]. While the global relevance of the Weddell Sea circulation is appreciated, its functioning and properties remain overall poorly constrained although it is clear that its properties are changing [56, 60–62]. Using hydrographic snapshots, [63] described the circulation in the Ross Sea, where the eastern boundary was determined to be controlled by the southward extension of the ACC core flowing through the Udintsev Fracture Zone. Gaining an appreciation of the Ross Sea circulation's large-scale variability, [51] used satellite altimetry to determine several modes of variability, and [64] highlighted how the overall region is seeing a long-term freshening. Satellite and Argo measurements are increasingly able to give a less static appreciation for variability in the Southern Ocean region, [13, 19, 65]. As one of the most remote areas on Earth, data acquisition is exceedingly difficult in the Southern Ocean [66], particularly in winter where accurate observations of the wind stress curl and current interactions would be particularly insightful. In effect, there is a lack of observations from one of the key regions shaping our climate, calling for an efficient use of resources, data, and research to advance knowledge. As demonstrated in the present work, machine learning is well placed to assist by determining where key dynamics are taking place and how they are dynamically connected.

The meridional overturning contribution

The idealised studies reviewed above largely do not take zonal variability into account with important implications for how applicable resultant conclusions regarding the overturning circulation are to the real ocean. The lack of zonal variability means that the deep isopycnals that upwell in the Southern Ocean, fuelling the overturning, are assumed to have a similar slope and subsequently exposed to similar surface forcing [12, 67–69]. This ignores the impact of gyre circulation, meanders of the ACC and the associated bathymetric variability. Recently, [70] highlighted further challenges using idealised channel-model frameworks, in that both topography and a residual overturning are necessary to understand even the basic role of wind forcing in the Southern Ocean.

The Southern Ocean circulation is implicated in the upwelling of deeper waters and gyres are particularly key for the doming of isopycnals. Previous work has noted the existence of a spiral structure in the Southern Ocean upwelling encircling the Antarctic continent [71, 72], and connected to topographic 'hotspots' [73]. Of note is that these are not confined to the narrow band directly to the south of the ACC meander as idealised studies could imply. The role of gyre circulation in the context of upwelling happening over a larger area remains unexplored. Note that within [71–73] the characterized processes are not confined to the traditional gyre regions of the Weddell and Ross seas, suggesting that more complex physical drivers are involved.

With a changing climate, models and future projections largely agree that the wind forcing in the Southern Ocean will increase [74]. Increased wind forcing is not expected to increase the volume transport of the ACC, which is limited by eddy saturation, but it is expected to intensify the overturning circulation [52, 74–76]. Where this intensification takes place will be dictated by where a bottom pressure torque dominated gyre circulation is present. If follows that understanding zonal heterogeneities are central to skillful projections. Using a breakdown by area of the gyres informed by objective determination of dynamical regimes, the distinct regions to focus on can be identified. With this insight, the associated impacts on, for example, melting through warm upwelled waters impacting continental ice shelves and the carbon budget can be estimated and more efficiently monitored.

Insight guided by machine learning

Understanding the interplay of the governing forces of ocean circulation, discovering in what areas certain driving forces are more prominent than others can focus work and accelerate insight, for example, as illustrated through the problematic nature of arbitrarily choosing gyre boundaries. Within physical systems ranging from the ocean and climate, through to general relativity and medicine, identifying subregimes in driving forces have driven progress by guiding intuition [25]. Unsupervised machine learning is well suited to finding subregimes, and can act objectively without human bias. The machine learning algorithm applied here is designed to be *interpretable*, which we define as the ability to trace exactly why the machine learning made its suggestions. Described in detail in [24, 77], the regime identification here was tailored to geoscientific application and in essence can be understood as identifying regions of statistically significant co-variance between equation terms, performing an empirical leading order analysis.

Here, the distinctions between the gyre-like circulations in the Southern Ocean are characterized as they are revealed using the dynamical regime method to highlight their areal boundaries. Then the Southern Ocean gyre circulation is discussed in more detail, specifically in the context of the distinctions between a friction and a bottom pressure torque dominated flow. The importance of defining the area selected objectively is highlighted. The specific circulation that the dynamical regimes highlight are discussed in terms of westward flow. The paper then illustrates how the dynamical regimes highlight where the contributions to the meridional overturning are found in terms of the frictional and bottom pressure torque dominated regions.

The present work highlights that not recognizing the important role played by the zonal extent of rough topography in the Southern Ocean, that stretches between the Weddell and Ross Sea, can lead to an underestimation of Southern Ocean overturning through neglecting key components. This implies that predictions of how and where upwelling may change in the future could be inaccurate. The conventional two-gyre view also presents a misinterpretation of the overall gyre-like circulation,where the circulation in the Weddell and

Ross Sea's are components of a system of connected sub-gyres. The presented results constitute an advance in the theoretical understanding of the gyre-like circulation and its role in the climate system, specifically also through recognizing the important confluence of different drivers of the circulation and their role in the overall semi-circumpolar circulation system. The quasi-circumpolar nature of the supergyre has implications for establishing observational platforms with a focus on upwelling, as these could be guided by the location of the sources of dissipation.

Results

The present paper presents the results of a machine learning assisted empirical leading order analysis performed on the global ECCOv4 state estimate. In the past, much progress was made analysing the equations describing ocean flow by linearization and simulation. However, the presence of nonlinearities have hindered, and even stalled, progress. Here, a clustering based machine learning methodology presented in Sonnewald et al. (2019) is used to guide hypothesis construction through an empirical leading order analysis of a closed set of equations as the output of the ECCOv4 global state estimate.

Global state estimate

The data used for the present analysis is from the ECCOv4 [78] global state estimate [79]. ECCOv4 has a nominal 1° resolution. The state estimate combines available data with a free running model, and is thus well suited for this study aiming to conceptually bridge the gap between the idealized and realistic numerical modeling studies. A least-squares with Lagrange multipliers approach is used to obtain observationally adjusted initial and boundary conditions as well as arrive at internal model parameters. This allows a free-running version of the MIT General Circulation Model (MITgcm, [80]) that has been optimized to follow observations. Adjoint methods are used to create the state estimate. Using the adjoint allows both the optimization to data, but also the closure of the momentum budget. The closeness to data is a particular benefit of using the state estimate, as other products may use ‘nudging’ terms to bring models closer to observations, which would not allow a sufficient closure of the momentum budget. This budget closure is seen as an important component of the success of the dynamical regime identification.

The global ECCOv4 model is preferred to a regional model, as this represents the global co-variance space given by the ocean dynamical drivers in a more consistent manner. This is because the unbalanced nature of the dataset, where those regions in co-variance space that do not account for a large percentage of the overall data, have more opportunity to be recognized as a coherent pattern rather than being classified as noise. The same dynamics are expected to be reflected in a global or regional model, but misclassification could be more prevalent as the less spatially dominant regimes could conflate the robust isolation of regimes, rendering the statistical model less significant. Work is ongoing on a higher resolution global dynamical regime identification effort, but is outside the scope of the present paper.

Identifying dynamical regimes: Interpretable machine learning

The question of understanding important distinction in the governing dynamics in the Southern Ocean is made difficult by the myriad of interacting driving forces. Conventionally, a hypothesis of dominant balances could be proposed and tested following expert intuition alone. Here, interpretable machine learning is used to establish hypotheses, in the form of distinct regimes within the driving forces. These regimes are spatially local parsimonious representations of the full equations, where the machine learning algorithm is used to determine where terms are negligible. Methods employed are chosen specifically to create an interpretable machine learning study.

The unsupervised machine learning clustering method k-means was employed to identify 2-dimensional dynamical regimes (Fig. 1a) in ECCOv4r3 time mean fields (1992-2013). Approached naively, finding robust dynamical regimes within the full momentum equations is likely intractable due to the high dimensionality of the complex numerical model, with a high likelihood of non-unique solutions conflating both arriving at a robust model and also interpretation. To facilitate interpretation, and reduce dimensionality, we initially employ an equation transform into the BV equation described above (see Supplementary A for more detail). The five terms of the BV equation form a closed budget, and a 5-dimensional vector field, $\mathbf{x}$, in each the model grid point with (longitude, latitude) $= (\theta, \phi)$. Designating an index i for each grid point, each element $\mathbf{x}_i$ is a 5-dimensional vector defined on the model's horizontal grid. Each index i now uniquely identifies a grid point on the sphere, with (longitude, latitude) $= (\theta, \phi)_i$. Within the data in $\mathbf{x}$, six distinct and statistically significant dynamical regimes are identified as clusters using the unsupervised machine learning k-means algorithm together with information criteria model selection (Akaike and Bayesian information criteria), and a specifically developed geographical area coverage criterion for oceanographic relevance. The method and workflow, in combination with working on a closed BV budget, was designed for interpretability, and to be appropriate for geoscientific application. The interpretability comes from the method being decomposable into separate steps, where the steps are humanly tractable, and using an algorithm that offers transparency through its simplicity and clarity of assumptions. The dynamical regimes were original presented in Sonnewald et al. (2019), where more details on the method can be found as well as extensive code and explanation in https://github.com/maikejulie/DNN4Cli.

The six dynamical regimes are back projected onto the globe, where the geographical area covered signifying where the unique balance of dynamical drivers is present. The regimes are described in detail in [24, 77], and here we restrict the description to the three regimes present south of 50°S (Fig. 1a). The global area averaged term balances (Fig. 1a) demonstrate which dynamical drivers are important and which are negligible. The 'Northern Hemisphere Sverdrupian' dynamical regime (N-SV, pink) represents a region where the vorticity input by the wind is largely negative, and that input by advection is positive. The N-SV regime will be referred to as the Sverdrupian regime for convenience. The 'Southern Ocean' dynamical regime (SO, gray) is found almost exclusively in the Southern Ocean. The topographic interactions through the bottom pressure torque are consistently a source of positive vorticity, as is the convective component. The wind stress curl balances the advective and topographic components providing negative vorticity. The SO forms a very strong topographic Sverdrup balance. The SO regime will also be referred to as the topographic Sverdrup regime to avoid confusion. The 'Non-linear' regime (NL, light blue), is associated with areas of rough bathymetry, such as ocean ridges and shelf breaks. It is particularly prevalent in the higher latitudes. The NL regime is notable as it is made up of a collection of smaller regimes that all have a large non-linear torque component, with varying sign, but make up a very small component of the ocean area [24]. Uniquely among the dynamical regimes, the non-linear regime has a notable non-linear component. The non-linear terms have a dissipative component, and have a unique role acting to steer the ACC and provide the necessary dissipation to allow gyre circulation.

The dynamical regimes

The regimes determined by the clustering analysis do not agree with the typical boundaries of the ACC and the classically recognized gyres in the Ross and Weddell Sea. Rather, a combination of dynamical regimes make up a quasi-circumpolar circulation spanning the region from the Weddell in the West to the Ross Sea in the East. The regimes prevalent in the Southern Ocean, are comprised of the Topographic Sverdrup, Sverdrup and Non-Linear regimes, referred to respectively as the SO, N-SV and NL regimes (Fig. 1). A distinguishing feature of the Southern Ocean is its circumpolar structure, also reflected in the dynamical regimes. The dynamical regimes largely form circles (moving away from Antarctica) of the SO, N-SV and NL regimes. Modulations to this are found in areas of rapid changes in topography, or along the Antarctic shelf where the NL regime is seen. Overall, the SO regime is seen south of the N-SV regime. This is a pattern seen to overall encircle the continent, with areas up and downstream of the Drake Passage (DP) offering the main break. The Campbell Plateau (the area between the Australia region and Antarctic continent, see Fig. 1) offers an area where the circular pattern of regimes is less clear, along with the Kerguelen Plateau and the Pacific-Antarctic ridge area. The geostrophic contours highlight why these discontinuities take place. The DP is the main area in the Southern Ocean where there are blocked geostrophic contours. The Campbell Plateau is an area where geostrophic contours are restricted.

Driving forces partitioned by regime

The driving forces, or sources of vorticity, of the dynamical regimes illustrate that the SO and N-SV are comparable in certain areas, and distinct from the NL regime (Fig. 2). The wind stress curl is largely positive southwards to approximately 56°S, and here there is a transition to negative wind stress curl, which progresses south to the Antarctic continent (Fig. 2a). Clockwise gyre circulation requires negative wind stress curl. The NL, SO and N-SV regimes derive negative vorticity from the wind stress curl, where the N-SV largely occupies the region where the wind stress curl is lowest in the Southern Ocean region (Fig. 2b), the SO regime is found exclusively in areas with larger negative wind stress curl (Fig. 2c). The NL regime does not occupy an area that is consistently negative or positive, and is found in regions where the wind stress curl has a large magnitude, either negative or positive (Fig. 2d).

The bottom pressure torque consistently has a large magnitude in the vicinity of bathymetric features, and overall contributes positive vorticity, with areas of negative vorticity input more local but with large magnitude (Fig. 2e). The N-SV regime has larger patches of negative and positive vorticity input seeming to alternate, but in the Weddell and Ross Sea largely positive values are found (Fig. 2f). A largely consistent positive contribution is found in the SO regime (Fig. 2g), with vorticity input becoming consistently more positive moving south. In the area covered by the NL regime, intense positive and negative values are found (Fig. 2h), with alternating patterns of positive/negative vorticity input. Areas of large bottom pressure torque are largely seen upstream of bathymetric obstacles and east of the DP.

The regions where large magnitude vorticity contribution are found in the bottom pressure torques, large non-linear contributions are often also found. The N-SV and SO regimes do not have large contributions from the non-linear terms ((Fig. 2n and o)), but the NL regime has marked contributions (Fig. 2p). Overall, the non-linear terms show few distinct patterns in the N-SV and SO regimes (2n, o).

The advective component is positive in the N-SV and SO regimes overall, and while the area averaged input of the NL regime is positive there is large variability (Fig. 2i). The overall advective component in the Southern Ocean is very similar in pattern to the bottom pressure torque (Fig. 2e), where large signals are found within the regions that have strong topographic variability. The N-SV and SO both have largely positive vorticity input by the advective component, although the N-SV has large negative areas for example in the Weddell Sea area (Fig. 2j and k). This is notable, as this is the same sign as the wind stress curl, implying that the balance here is not determined not on the basis of the advective component. These larger negative areas are overall absent in the SO regime, where the regime shifts just west of the N-SV regime to become positive entering the SO regime.

In general for the physical drivers, areas that stand out include the Pacific-Antarctic ridge where a large positive area in bottom pressure torque is seen before the ridge where the ACC spins up and is deflected north, and a negative area downstream. Similarly, the Scotia ridge and the Kerguelen and Campbell Plateau stand out as areas of large positive and negative sources of vorticity from bottom pressure torque. The decomposition into the dynamical regimes is seen to have intense regions isolated somewhat to the areas of the NL regime both for bottom pressure torque and non-linear vorticity (Fig. 2h and 2p respectively), with the less impacted areas in the N-SV and SO regimes (Fig. 2f, g and 2n, o respectively). Within the bottom pressure torque and advective component there seems to be compensation in the NL regime, with strong positive/negative bottom pressure torque appearing in areas where the advective component is strongly negative/positive. This is as expected.

The flow partitioned by regime

The flow partitioned into dynamical regimes shows that regions associated with different configurations of dominant drivers result in different flow patterns. The clear mapping between circulation and dynamical regimes is a highly novel achievement of unsupervised machine learning. The differences in the flow as delineated by the dynamical regimes is described starting from the bottom layers shown as a quiver plot overlaid with the dynamical regimes and geostrophic contours (below 4264m, bottom five grid cells, Fig. 4). To further reveal structures in the flow, sections across regions of interest in zonal flow, bottom pressure torque, non-linear torque and dynamical regime are presented below (Fig. 5). The overall structure seen is that in areas where the NL regime is present the flow has a large magnitude (Fig. 4), for example tracing the Pacific Antarctic ridge up until 130°E (Fig. 4a). The N-SV regime sees flow that has an eastward component or a small magnitude, as compared to the NL regime. An exception is seen in the Western region of the Weddell Sea where the N-SV regime has a large magnitude westwards and northward flow (Fig. 4b). Within the SO regime, a southward pivot of the flow, small magnitude or westward flow is largely seen such as from 170 to 140°W (Fig. 4a) and to a lesser extent in patterns within the region 20°W to 140°E (Fig. 4a, c and d). The tendency towards Westwards flow is particularly evident in the Weddell Sea area (Fig. 4b). It is notable, that even in the areas such as the Campbell Plateau south of Australia (169°E, 52°S, Fig. 1a), that forms a considerable topographic obstacle, there is no distinct southward flow as would be expected for the eastern terminus of a classical gyre structure. However, a distinct southward flow is seen at the eastern edge of the Ross Sea around 140°W (Fig. 4a). Instead, a gradual southward transition is seen throughout owing to topography, in contrast to the distinctly southward flow of the eastern terminus of the gyre past the Ross Sea. What distinguishes the Ross Sea area is that the Pacific-Antarctic ridge to its northwest is the last major topographic obstacle of the ACC before the DP. Here, between approximately 140-180°W (Fig. 4a) there are no features of bathymetry significant enough to induce large non-linearities, and provide sources of dissipation/sinks of vorticity. The geostrophic contours as a result are largely zonal, and the ACC follows these contours. The lack of a source of dissipation is significant because it allows the ACC to flow largely eastward without. Additional figures illustrating the ACC location and flow interactions with the non-linear at bottom pressure torque terms are discussed in Supplementary D (Figs. D1-D3)

Assessing key areas of interest looking at meridional transects (Fig. 5), the region after clearing the Ross Sea is seen to have a comparatively baroclinic zonal flow, meaning that it is concentrated at the surface and spread over a larger latitudinal band (Fig. 5a). This circulation is confined to the N-SV and SO regimes, illustrated in the strip of colours above each figure panel, and the bottom pressure torque and non-linear contributions are not very large. Moving into the Atlantic sector of the Southern Ocean (Fig. 5b), the ACC is more concentrated latitudinally, has a larger magnitude, and is split into two jets to the north of the two topographic obstacles. Peaks in the non-linear contributions are concurrent with these jets, mirrored by the bottom pressure torque. This latitudinal band is found in the NL regime. To the south there is a wide area of the SO regime. Here the zonal flow is very small just south of the NL regime, and moving south reverses direction to be westward. The flow has a barotropic structure and the non-linear and bottom pressure torque contributions are small. Notably, the zonal flow becomes smaller moving southwards, and a distinct new band of relatively intense westward flow with a clear surface-concentrated structure is found in the NL regime encircling the Antarctic continent.

There is an interesting structure in depth that is connected to the dynamical regimes. Overall in the surface, the ACC dominates the flow, and is largely confined to the NL regime. Here, relatively barotropic intensification of the flow is evident when interactions with topography occur. In terms of providing a ‘dynamical western boundary’, the dissipation required is presumably found in the non-linear term that characterize the NL regime, which is the only dissipative term in the BV equation, as suggested by [30]. The pattern of bottom pressure torque and non-linear terms are seen to span the Southern Ocean in an almost circumpolar fashion. Areas where the NL regime leaves only limited latitudinal gaps, such as around the Kerguelen (≈75°E) and Campbell Plateaus (≈170°E), as well as the Pacific-Antarctic ridge (≈140-180°E), the geostrophic contours are non-zonal. Here, the ACC becomes intensely barotropic, and is wont to split up into multiple jets, seemingly in response to topographic variability. Passing through the Kerguelen plateau (Fig. D5c), the N-SV regime is less present, but within the SO regime a southward and westwards deep circulation is maintained. Passing over and through the Campbell Plateau (Fig. D5d), there is a region where there is no such deep circulation. Here, the ACC first intensifies as it is being directed North, and then relaxes as it flows along geostrophic contours (Fig. D5a). The ridge geometry in this area is complex, but as the ACC is traveling north, a westward flow appears. This westwards flow is part of a clockwise circulation in the Ross Sea area, confined to the eastern edge of the Pacific Antarctic Ridge.

The lateral and vertical extent of the ridge is interpreted as playing a role in the resultant flow. For example, in the Ross Sea a clockwise circulation is seen at depths deeper than 3 km. The implication is that the physical barrier is 'blocking' the flow at this depth, but not above it. As such, a rotation of the flow with depth is expected, and that this would be proportional to the topographic obstacle and strength of the flow it impedes (expressed as the pressure gradient across the topographic obstacle). Here, further analysis of specific ridge geometry interactions with the deep ocean flow is out of scope.

Contributions to the overturning streamfunction by regime

The differing balances of forces in the dynamical regimes impact their contribution to the global overturning, described as a zonal streamfunction (Ψ, Fig. 6a, Supplementary C). Here, the density of the water masses are used as our frame of reference, illustrating what class of water is transformed. The meridional overturning circulation captures the bulk meridional movement of watermasses at a fixed latitude. As a large-scale circulation, the global overturning has clockwise (red) and counterclockwise (blue) features. While the Southern Ocean is our focus, the global circulation will be briefly described for completeness. The light surface waters (down to $\approx 35\sigma_2$ and 30° of the equator) form a clockwise surface cell in the Northern Hemisphere, and a counterclockwise circulation in the Southern Hemisphere. In the denser water-masses that are $\approx > 35\sigma_2$ and north of ≈60°S there is a clockwise circulation that stretches to the high northern latitudes, where the dense waters that feed its lower component are created. In the Southern higher latitudes, the loop is closed through upwelling, where the wind gyres are implicated.

In the Southern Ocean, the circulation has a predominant counter clockwise feature (Fig. 6b). This shows surface waters that are less dense becoming denser moving southwards, where beyond 60°S the circulation appears to be entirely counter clockwise. There is also a line of counter clockwise deep circulation in the densest waters stretching North, reaching beyond 25°N. The water masses in this bottom circulation are some of the densest in the ocean, and are formed in the high latitudes, by transformation of the waters brought up from the intermediate depths. The individual dynamical regimes' contributions to the Southern Ocean branch of the overturning can be assessed by decomposing the overall transport by dynamical regime, and calculating the individual components as done in [77]. The sum of the individual components add up to the overall streamfunction, and are here used to highlight the compensation between components and are suggestive of what overall work is done by respective regimes. Note the component of the streamfunction in each regime does *not* individually represent a streamfunction as Helmholtz' theorem is not strictly satisfied, and a residual may be present but is assumed to be small south of the ACC meanders (Supplementary C).

Decomposing the overturning into dynamical regimes (Fig. 6c, d, and e) shows the local contribution of each regime individually, revealing a complex interplay of dynamical features and compensation between them. The focus is on the SO, NL and N-SV regimes as they cover most of the area. Overarching coherent and in-depth physical regimes emerge (Fig. 6). The global overturning is calculated zonally, which means that the compensation and local circulation can be missed. The SO regime accounts for the largest part of the clockwise circulation south of ≈55°S (Fig. 6c). It reaches waters that are as dense as $\approx 37.25\sigma_2$. The N-SV regime is also largely clockwise north of ≈60°S (Fig, 6d). The circulation reaches less dense waters than the SO regime, and is less intense, particularly south of ≈57°S. South of ≈63°S, a counterclockwise component appears. The clockwise circulation in the SO and N-SV is further confirmed by the upwards movement of water seen in the vertical velocity (Fig. 7b and c). The NL regime shows a pronounced counterclockwise circulation (Fig. 6e). The counter clockwise circulation is at its strongest between ≈50°S and ≈67°S, moving south of which it briefly becomes clockwise, disappears and then resumes as counterclockwise. The southernmost feature is due to the transformation along the Antarctic continent, seen as the band of negative vertical movement (Fig. 7d). There is also an upwards component, but the downwards w component dominates. The SO and N-SV regimes comprise areas that are dynamically more consistent, with the bottom pressure torque,

$\nabla \times \tau$ and the advective component having more consistent signs.

To conclude the results section, an overall sketch of the concepts is presented in Fig. 8. The ACC is moving eastwards (NL, light blue on bottom and big arrow in 3D rendition in Fig. 8) creating a source of dissipation as a bathymetric obstacle is met (Fig. 8, brown bump), deflecting the flow north (Fig. 8, big arrow veering right). If enough of a change in vorticity/dissipation is given by the topography/flow interaction, a southward change in flow direction is seen that interacts directly with topography (Fig. 8, small arrow). A clockwise lateral circulation arises following the obstacle, as the gyre-like circulation (SO and N-SV regimes in gray and pink). The impact on vertical flow and isopycnals is that the ACC is seen where the isopycnals are steep, and in the SO regime the upwelling flow is seen. Implied, but not directly depicted is that one has a distinct eastern and well-defined boundary where there is no topographic obstacle impeding the ACC.

Discussion

The dynamics in the Southern Ocean are uniquely important for understanding the world's climate, as it acts to connect the world ocean and close the loop for the global meridional overturning circulation. In the present paper, the gyre-like circulation in the Southern Ocean is discussed and the conventional view of two separate sub-polar gyre systems is challenged, with implications for how the upwelling is realised. The importance on zonal heterogeneity is stressed, especially in relation to conventional idealised frameworks. A novel unifying supergyre framework is put forward, extending southwards of the dynamical western boundary imposed by the ACC, enveloping both traditionally recognized circulation structures and the in-situ observed circulation in-between (Fig. 9). The limited observations available suggest agreement, particularly in the poorly studied area eastwards of the Weddell Sea [13, 14, 18–23]. Simulation of gyre structures in both idealised and realistic models is challenging [7], with the implication that model representations of dynamics key to sea level, heat and carbon storage variability could be fundamentally misrepresented, and our understanding of how it may change in the future could be skewed. Despite the key importance of Southern Ocean circulation, large biases between climate models persist, highlighting the need for increased fundamental understanding of how the circulation is realized in realistic model settings [4]. This work stresses that gyre-like circulation in the Southern Ocean is uniquely implicated in the upwelling and thus the maintenance of the meridional overturning circulation, particularly in regions where the gyre circulation is given as a strong topographic Sverdrup balance (a balance between the wind stress curl, bottom pressure torque and advection). The importance and widespread nature of the topographic Sverdrup balance implies a fundamental role for bathymetric interactions well beyond the major ridges that induce the meanders of the ACC. The remainder of the discussion is structured as follows. First, we define and describe the quasi circumpolar supergyre of the Southern Ocean. Then these results are discussed in the context of existing work, in particular regarding ocean observations. The role of upwelling and the southern closure of the global overturning circulation are then discussed, before setting the novel framework into the context of the global climate and providing guidance for a future framework for observation strategy. The last section concludes the paper.

The quasi-circumpolar supergyre of the Southern Ocean: Scaffolding by topography

In contrast to wind gyres in the subtropical Northern Hemisphere, no continental western boundary is present to act as a sink of vorticity/source of dissipation in the subpolar Southern Hemisphere. The topographic obstacles present in the Southern Ocean act to impede the Antarctic Circumpolar Current (ACC), and provide a 'dynamical west' that allows gyre circulation to develop to the south of the ACC-induced dissipation of vorticity [30]. As such, gyre circulation develops in the lee of topographic obstacles that force the ACC north, appearing as a southward bend of the flow (much weaker than the ACC) or even reversal to travel westwards. A distinct 'eastern boundary' in the form of a continent is also not present, and only in the area where no significant topographic obstacles are seen, and the ACC becomes comparatively baroclinic following geostrophic contours (we describe this as a quasi-linear-free mode), is there a distinct end to the supergyre. This eastern boundary is seen as a relatively well-defined continuous current moving south.

We suggest that the gyre-like circulation in the Southern Ocean is quasi-circumpolar, absent only where the circulation switches to a quasi-linear-free mode that is minimally impeded by topographic obstacles to the West of the DP. What is presented here as the gyre structure departs from the normally discussed Weddell and Ross gyres. The suggested framework results in a quasi-circumpolar circulation that envelops the traditionally defined Weddell and Ross gyres, with considerable leakage across regimes, and defines the eastern gyre terminus as the region where dissipation source provided by rough topography *ends* (Fig. 9).

The sink of vorticity of the ACC as it interacts with topography supports a gyre-like circulation. Here, we suggest that this dissipation, and the areas where dissipation happens, can be seen as 'scaffolding' maintaining the supergyre. The present paper suggests a more useful description would be given by identifying regions that can provide such structure by acting as sinks of vorticity. Topographic obstacles act as sources of dissipation, effectively being scaffolding to the quasi-circumpolar supergyre, and elongating the dynamical western-boundary zonally following south of the ACC. The scaffolding supports the elongated structure of the gyre while allowing for a gradual southward and even westward transition of the flow within the localized sub-gyres. Without this scaffolding, the quasi-circumpolar gyre would collapse, and the localized sub-polar gyres could be considered as separate entities. In the presence of the ACC, the concept of distinct, continental-scale boundaries would suggest that areas providing some latitudinal obstacles such as the Campbell Plateau could act as eastern boundaries. Here it is suggested that areas such as the Campbell Plateau should be interpreted as part of the scaffolding: a latitudinal excursion and merely a continuation of the dynamical western boundary. As such, the *end of the source of dissipation* is the relevant bounding topographic structure in the Southern Ocean, and the location where there is no longer a topographic obstacle of a scale that can support a sufficient pressure gradient should be seen as the *terminus* of the gyre-circulation that starts after the DP. The implication of this, for example, is that studying the circulation in the Weddell Sea in isolation would not be faithfully represented without also representing larger gyre-like system it is part of as model boundary conditions. Effectively, the individual sub-gyres could not exist in isolation. The interaction of the ACC with the present topography maintains the required lateral pressure gradients that support the gyre-like structure, owing to the prior dissipation further upstream (which could be considered a pre-cursor of the resulting circulation).

The gyre-like circulation consists of a flow where the portion of the clockwise circulation headed north is well defined, but the southward portion is less so. Downstream of the DP and associated Scotia ridge, such a northward portion of a clockwise circulation is found in the Weddell Sea reaching down to depths below three km. The Campbell Plateau and associated Pacific-Antarctic ridge are also able to maintain a pressure gradient, but to a much smaller extent, with a circulation that only forms below three km. The pressure gradient in these regions establishes a local effective eastern boundary below 3 km, whereas the ultimate eastern terminus of the supergyre is a result of a lack of topographic obstacles. The areas where the gyre-like flow fails to form a well-defined return flow are identified as distinct dynamical regime that is in a topographic Sverdrup balance (SO), where the bottom pressure torque and the advective component contribute positive vorticity, while the wind stress curl balances this, adding negative vorticity. Broadly, there is a regime in Sverdrup balance (N-SV) to the north of the SO regime, where the bottom pressure torque is less consistently strong and the flow is more baroclinic, and is largely associated with more zonal flow. The ACC is consistently seen as occupying the dynamical regime that stands out for its non-linear vorticity contribution (NL regime). This is expected, also because the non-linear terms include a dissipative component, that provide the sink of vorticity needed for gyre-like flow.

The role of upwelling and the southern closure of the global overturning circulation

The upwelling of warm water, and doming of isopycnals, is seen to take place in a band that approximately encircles the Antarctic continent, largely given by the SO dynamical regime. An exception is seen upstream of the drake passage (DP) where the flow follows geostrophic contours as no major topographic obstacles are present. The upwelling is distributed across, and brings up the densest waters, in the areas dominated by a topographic Sverdrup balance in the SO dynamical regime. This offers support for the hypothesis put forth by [72], where areas associated with more energetic areas of the flow produce upwelling downstream.

The overturning streamfunction in the Southern Ocean has distinct contributions from the different dynamical regimes, as revealed by the breakdown of the overall streamfunction (Fig. 6). The SO regime contributes the major fraction of the deep warm waters brought up from depth, which is expressed as a clockwise (Fig. 6) circulation. The N-SV regime also contributes in a clockwise fashion, but is situated in less dense waters with a less vigorous overturning. The NL regime provides the main counter-clockwise contribution to the overall streamfunction. The counter-clockwise contribution of waters spanning a large range of densities is consistent with the NL regime being the area where the warm deeper waters brought up by the SO regime release their heat, become dense and sink. The view that the upwelling is contributed within the SO regime, that covers a large area, is concurrent with the proposed paradigm shift towards seeing the upwelling in the Southern Ocean as a 'spiral staircase' rather than localized features [71, 72], which were also associated with areas of negative wind stress curl. The suggestion that the upwelling happens in an upwards spiraling fashion has implications for the processes leading to the upwelling. Note that the supergyre framework is described in a tempoally averaged sense in the present manuscript. The supergyre framework does not dictate that a parcel of water moving vertically and being transformed in an area covered by the SO regime cannot continue into a different regime and predominantly stay within this density class as it moves zonally. The supergyre framework does suggest that the upwelling and transformation happens over larger areas downstream of topographic obstacles.

The supergyre in context of available observations

The supergyre framework constitutes an advance in understanding of how gyre circulation arises in the Southern Ocean in association with the ACC's interactions with topography, positing that a supergyre circulation encompasses the Weddell and Ross Sea's and the area in between. The supergyre framework is distinct from the idea that the ACC is the Eastwards Northern edge of the gyre and the Antarctic Shelf Current is its Southern branch. Rather, the ACC is a dynamical western boundary where dissipation is sufficient to induce a gyre-like circulation. In the supergyre framework, the important role of topography starting from the Weddell Sea and reaching Eastwards to the Ross basins is highlighted. Here, we highlight three key predictions from this novel framework: 1) there is only one concrete end of the supergyre dictated by the lack of rough topography, 2) multiple sub-gyre or gyre-like circulations will span the entire area and 3) CDW waters, that are an important result of gyre-like flow, will reflect the complex circulation patterns.

First, the supergyre framework predicts that the main concrete *end* of the gyre, defined as lacking a continued initiation of clockwise flow induced by topography, should be after the Ross Sea. An Argo float-derived stream function depicting the horizontal circulation of the Weddell Sea, presented in [13], highlights the topographically induced baroclinic shear at the open boundary of an eastern sub-gyre, in contrast to a barotropic western sub-gyre where topography plays a lesser role in comparison to wind stress and advection. Further confirmation of a lack of a concrete Eastern Boundary of the Weddell Sea gyre-like circulation comes from [14], who used hydrographic measurements using conductivity, temperature and depth (CTD) profiles and acoustic Doppler current profilers (ADCP) to describe the role of the southwest Indian Ridge in increasing instabilities of the ACC that were hypothesized to drive an intense mesoscale eddy field rather than a defined Eastern Boundary Current. [18] similarly suggested a significant presence of mesoscale eddies, rather than a well-defined flow to the South.

Second, if useful as a conceptual model, the supergyre framework suggests that further gyre-like circulation should exist where significant dissipation happens, such as, the Indian section of the Southern Ocean (Fig. 4). [22] used two sections from the World Ocean Circulation Hydrographic Program to highlight the complex circulation between Australia and Antarctica with substantial gyre systems. [19] used more detailed Argo data from the Australian Antarctic Basin to show what the Authors refer to as 'sub-gyres'. The sub-gyres are associated with a movement of the southernmost jet of the ACC, and a southward excursion of CDW with active cross-slope exchange between isobaths occurs. [19] find that bathymetry determines the structure of the gyre, and a combination of transport and topographically controlled mean flow and eddy transport. Using hydrography and drifters, several studies have pointed to a gyre-like circulation in the Prydz Bay area (70 and 80°E) [23, 54, 55, 81], and also around 90 to 115°E [23]. Similarly, a single gyre (80 and 110°E) in the Australian–Antarctic basin with eddies to the East is proposed by [82] in model output, and verified against iceberg trajectories and Argo floats. In contrast, no gyre-like circulation is reported Eastwards of the Ross Sea to the Author's' knowledge. The observational estimates spanning from the Weddell to the Ross Sea highlight that there is copious cyclonic circulation. The observational studies do not share a dynamical definition of a 'gyre' beyond being a cyclonic circulation south of the ACC. However, we note that where reported the gyre-like circulation is largely in lee of a topographic obstacle where the ACC, or one of its jets, veers North providing a source of dissipation. Due to the sparsity of observations, the presence of distinct southward return flows are not present in literature to the Author's knowledge, which also appears in support of the supergyre framework.

Third, the Southern Ocean's role in the southern limb of the overturning circulation through upwelling can be interpreted as emerging from sub-gyres within the structure of a much larger supergyre. The CDW waters are of particular importance to the upwelling, and are roughly bounded by topographic features and make up over 50% of the Southern Ocean volume [83]. The CDW is known to have a very complex pattern of origins, and are distinct from more traceable watermasses such as North Atlantic Deep Water. The complexity of the CDW is well aligned with the supergyre framework, as contributions through upwelling would come from the sub-gyres in association with bathymetric obstacles. To have upwelling, there needs to be transport across the ACC front, and there is likely cross front transport where you have a gyre forming to the South. This could happen through bathymetric dissipation leading to eddy activity (inducing southward transport, [84]) in combination with negative wind stress curl (surface northwards). Given this, the supergyre framework would predict that the CDW will have several sources and cross the ACC front downstream of locations associated with non-linear term dominance. To date, no observations or specific modeling studies exist exploring such mechanisms in the context of gyre circulation. However, lagrangian particle tracking experiments in high resolution models are interpreted as supporting the supergyre framework. [72] present a compelling analysis suggesting that energetic regions associated with topography played important roles in bring water parcels upwards on a spiraling pathway around the Southern Ocean. Focusing on the upwelling of carbon, [85] shows a similar relationship with topography, but only considers the location where a particle crosses 1000m and discards the areas associated with sea ice. Both [72, 85] do not consider the upwelled volume and may not have time integrations long enough to capture the impact of the circulation in areas with longer residence times like the Weddell and Ross Seas. Future work assessing the upwelled volume of CDW waters using a lagrangian framework could offer fruitful insight.

Our study uses the state estimate (ECCO), which offers the closest product that can act as a comprehensive observational dataset capable of closing budgets of vorticity. We note that the low resolution of the state estimate means that direct comparisons to observational data is difficult. In particular, while the overall impact of the mesoscale eddy field is present in the observations used to constrain the ECCOv4 state estimate, the associated upwelling in ECCOv4 will be spread out due to the necessary parameterization. As such, the present paper offers context for higher resolution models such as [72, 85]. However, compared to observations ECCOv4 is seen to reproduce watermass structures well [86], suggesting that the dynamical regimes and their gross representation of upwelling structure and location are reasonable. The present paper suggest that more observations are needed, particularly as deep waters have been observed to take concrete and localized *advective* pathways identified in [18, 61, 87, 88] which would not be represented in ECCOv4. The developed framework also neglects thermodynamic drivers of the upwelling and subsequent water mass transformation.

A potential new framework for monitoring and assisting observational efforts

When observing the ocean in-situ its sheer size offers a formidable challenge. Where is data needed, and at what temporal and spatial resolution? At high latitudes, small length and time scales become necessary due to the Rossby radius, and lead to a still pressing lack of observational data. With rapid observed changes in the ACC's polar front and associated CDW implications, improving frameworks for observational support are increasingly important [20]. The notion that one supergyre spans the Southern Ocean with distinct dynamical regimes contributing to the upwelling of deep warm waters suggests that the treatment of the Weddell and Ross Sea circulation patterns as distinct gyres could be misleading, and may underestimate the amount of upwelling happening as this is dispersed across large areas. The results presented here emphasize the benefits that continuous float measurement could offer, and that greater areal coverage concentrated within the southeast of obstacles could be fruitful, for example, in combination with acoustic mooring arrays. However, note that while the presented results are based on a state estimate, a model fit to observations, the low resolution would not be able to capture advective processes that are more localized.

For observing gyre circulation and associated upwelling, the present framework has the potential to contribute to a targeted data collection strategy both conceptually and more practically. Fundamentally, much theory is still formulated in two-dimensions, and far removed from the three dimensional realistic frameworks needed for supporting observations. Here, by highlighting the key role of dissipation in upholding the scaffolding of the proposed Southern Ocean supergyre, observations could be guided to regions with specific topographic properties and associated wind stress patterns to the South. We note two inferences that could be of interest when designing monitoring or in-situ observational efforts. Firstly, the ACC, interpreted as a dynamical construct that constitutes a source of dissipation rather than defining it by its fronts, could help indicate areas where isopycnals may be heaving to the southwest. This definition of the ACC could perhaps be more related to the pressure gradient across bathymetric obstacles and their impact on the flow to the southeast of the obstacle. Second, within the supergyre framework, knowing where the SO dynamical regime is present can help target observations. Inferring the dynamical regimes was pioneered in [77], effectively providing subsurface inference based on surface wind stress curl, sea surface height and the static depth field. The presented results stress the important role of the wind stress curl, as this is a defining driver of the topographic Sverdrup balance regime. The wind stress curl is known to intensify with a warming climate [89], but specific implications for the CDW are still unclear [20]. Here, [77] could be used to guide and infer changes, for example, in spatial regions associated with CDW upwelling locations as driving forces change with global heating.

On large timescales, the presence or absence of boundaries allowing a circumpolar flow within the Southern Ocean is known to have an influence of the global climate. On geological timescales, the bathymetric configurations in the ocean can change, for example closing the DP or the Tasmanian Gateway between Antarctica and Australia. The changes in the continental configuration lead to distinct gyre formation to the east of the obstacles, and strengthen the poleward heat transport [90, 91]. Consequently, it is the strength of the gyre circulation, not the strength of the ACC that sets the meridional transport of heat, in agreement with the conclusions presented here. This causal relationship between the ACC, gyre circulation and the heat transport has been highlighted in the paleo literature as resolving a delayed onset of the strong ACC [92–94], as it was the weakening of the gyres that allowed the changes in heat transport, rather than the strengthening of the ACC. With a likely strengthening of the wind stress curl under a future climate [89], it is notable that the gyre circulation will likely spin-up and the southern branch of the meridional overturning strengthen, rather than the ACC volume transport, would increase [52, 74–76]. As such, the connection between the ACC and the wind gyre circulation in the Southern Ocean can be expressed in terms of the *present day* gyre circulation being contingent on the ACC.

Conclusion

This study utilized classic machine learning in combination with oceanographic theory, to create an interpretable machine learning analysis of both the nature of gyre circulation in the Southern Ocean and its fundamental role in the closure of the southern limb of the meridional overturning circulation. Concretely, machine learning was used to pose hypotheses of what regions were dynamically distinct, and thus have distinct impacts on the circulation. The machine learning used is concretely chosen to be both geoscientifically relevant through specifically designed model selection criteria, and to be interpretable in that the entire process is tractable. Fundamentally, machine learning was used for hypothesis building, similar to the classical use of physical intuition, enabling the analysis of highly complex and nonlinear data. Similar applications of machine learning as a tool for empirical leading order analysis is ideally placed to accelerate discovery within oceanography and beyond [24, 25]. Specifically within the context of understanding the dynamical balances within gyre circulation, [42] highlights the impact that the choice of geographic area within which to assess the dynamical balances matters. While previously looking along streamlines was used to make progress, here the objective dynamical regime discovery allowed the analysis to be guided by statistically significant configurations of drivers.

The findings presented demonstrate that the nature of gyre circulation in the Southern Ocean differs distinctly from classical gyre theory and the conventional view of two seperate gyres in the Weddell and Ross seas, with observational estimates in support of the supergyre framework. The ACC acts as the sink of vorticity, relieving the need for blocked geostrophic contours, and a lack of a physical eastern boundary suggests that the gyre circulation initiated downstream of the Drake passage does not terminate, but is upheld through topographic scaffolding that continues to the Ross Sea. This topographic scaffolding allows a topographic Sverdrup balance regime almost encircling the Antarctic continent. This topographic Sverdrup balance regime accounts for the majority of the upwelling of warm waters that release their heat to sink and supply the lower limb of the meridional overturning. A benefit of the presented framework and approach is that we can address the zonal heterogeneity seen, for example, in warming trends. Conventional theory uses idealised and largely two-dimensional zonally averaged frameworks. Interpreted using this framework, the limited available observations suggest agreement. Results have important implications for monitoring strategies, that could crucially underestimate upwelling unless encompassing the quasi-circumpolar gyre circulation. Underestimation of the overall upwelling needs to be resolved if we are to truly comprehend the role of the Southern Ocean in redistributing heat and carbon in the context of global anthropogenic climate change.

Acknowledgments and author contributions

The author contributions are as follows: MS conceived of the experiments, performed the analysis and wrote the manuscript. KAR and RL reviewed and contributed to editing the manuscript.

The authors are grateful for valuable discussions with S. Griffies, V. Balaji, A. Adcroft, L. Talley, Y. Nakayama, D. Jones, J. Deshayes and I. Rosso. Y. Cho offered assistance with Fig. 3 and 8. MS funding: Cooperative Institute for Modeling the Earth System, Princeton University, under Award NA18OAR4320123 from the National Oceanic and Atmospheric Administration, U.S. Department of Commerce. The statements, findings, conclusions, and recommendations are those of the authors and do not necessarily reflect the views of Princeton University, the National Oceanic and Atmospheric Administration, or the U.S. Department of Commerce. RL funding: The Make Our Planet Great Again (MOPGA) funding from the Agence National de Recherche under the "Investissements d'avenir" program with the reference ANR-17-MPGA-0010. KAR funding: Project WedUP: Weddell Gyre Upwelling and Dynamical Processes funded by the Deutsche Forschungsgemeinschaft Schwerpunktprogramm SPP1158 Antarktisforschung, with grant number 424330345. Code is available through GitHub https://github.com/maikejulie/DNN4Clim and fully reproducible also within the Amazon Cloud. ECCOv4r3 data available at: https://ecco-group.org/products.htm.

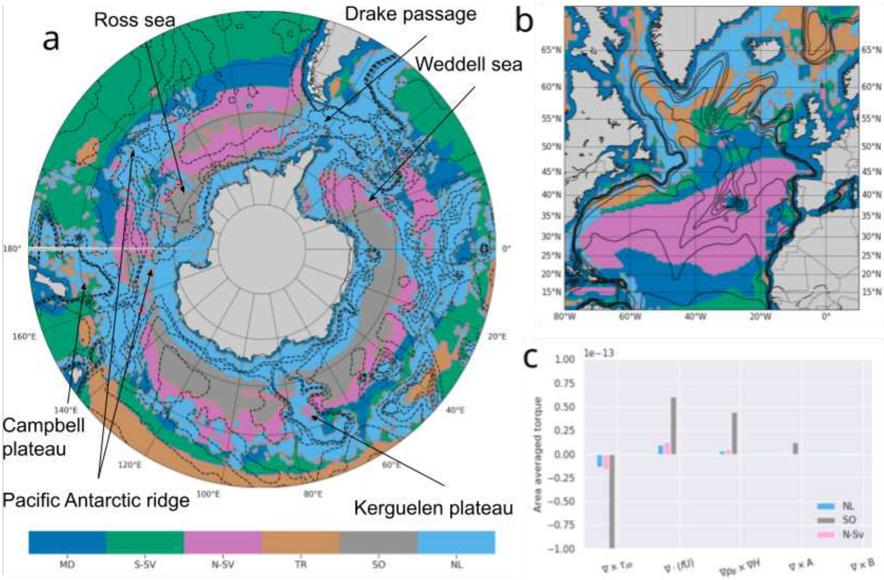

Fig. 1 Dynamical regimes in the Southern Ocean and subtropical North Atlantic. Panel a illustrates the dynamical regimes focused on the Southern Ocean from 40° southwards to illustrate landmass locations. Note the semi-circumpolar nature of the regimes. The regimes are global and discussed fully in [24, 77], where the momentum driven (MD, blue), Southern Hemisphere Sverdrupian (S-SV, green), Northern Hemisphere Sverdrupian (N-SV, pink), transitional (TR, orange), Southern Ocean (SO, grey) and non-linear (NL, light blue) regimes correspond to local parsimonious representations of the barotropic vorticity equation. Panel b shows the dynamical regimes for the subtropical North Atlantic. Panel c illustrates area averaged barotropic vorticity contributions of various terms for the SO, N-SV and NL dynamical regimes that are the current focus, discussed in the methods section. The contours are the geostrophic contours. Note the location of the NL regimes, associated with the Antarctic Circumpolar Current, and the area of bathymetric obstacles as illustrated by the geostrophic contours. labels highlight features discussed in the paper.

Supplementary information.

Appendix A Equation transform

To arrive at the five dimensional field from the full 3D model fields, a closed momentum budget was used. The discussion below is adapted from Sonnewald et al. (2019). The momentum and continuity equations of the ocean are seen as a thin shell sitting on a rotating sphere:

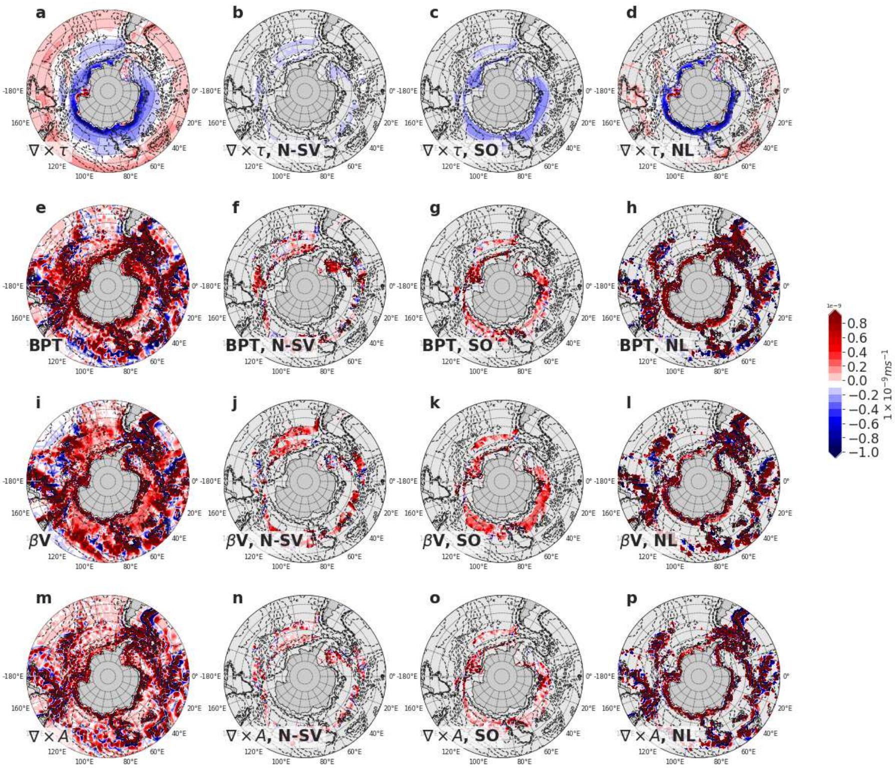

Fig. 2 The terms of the barotropic vorticity equation centered on the Southern Ocean. The first row (a-d) represent the wind stress curn ($\nabla \times \tau$). The second row from the top show the bottom pressure torque (e-h, BPT). The third row from the top represents the advective component of the flow (i-l, $\beta \mathbf{V}$). The bottom row represents the curl of the non-linear terms (m-p, $\nabla \times \mathbf{A}$). The portions in columns two to four anr broken down by dynamical regime. The first column a shows the full region, column two the N-SV regime, column three the SO regime and column four the NL regime.

$$\partial_t \mathrm{u} + f\mathrm{k} \times \mathrm{u} = -\frac{1}{\rho_0}\nabla_h \mathrm{p} + \frac{1}{\rho_0}\partial_z \tau + \mathrm{a} + \mathrm{b}, \partial_z \mathrm{p} = -\mathrm{g}\rho \tag{A1}$$

$$\nabla_h \cdot \mathrm{u} + \partial_z w = 0, \tag{A2}$$

Pressure, gravity, density, and vertical shear stress are p, g, ρ, and τ, respectively, with ρ_0 the reference density; the three-dimensional velocity field $\mathbf{v} =$ (u, v, w) $=$ ($\mathbf{u}$, w); the gradient $\nabla = (\nabla_h, \partial z)$; the unit vector is denoted

k; planetary vorticity is a function of latitude θ in $f\mathrm{k} = (0, 0, 2\Omega \sin(\theta))$; the viscous forcing from vertical shear is $\partial_z \tau$; the nonlinear torque is **a**, and the horizontal viscous forcing **b** includes subgrid-scale parameterizations. Under steady state, the vertical integral from the surface $z = \eta(x, y, t)$ to the water depth below the surface $z = H(x, y)$ is

$$\beta V = \frac{1}{\rho_0} \nabla \mathrm{p}_b \times \nabla H + \frac{1}{\rho_0} \nabla \times \tau + \nabla \times \mathbf{A} + \nabla \times \mathbf{B} \tag{A3}$$

where $\nabla \mathrm{U} = 0$, $\mathrm{U} \cdot \nabla f = \beta V$, the bottom pressure is denoted p_b, $\mathrm{A} = \int_H^\eta \mathrm{a} dz$, and $\mathrm{B} = \int_H^\eta \mathrm{b} dz$. The curl operator $\nabla\times$ produces a scalar, that represents the vertical component of the operator. The left-hand side of equation 3 is the planetary vorticity advection term, while the right-hand side of equation 3 is the bottom pressure torque (BPT), the wind and bottom stress curl, the nonlinear torque, and the viscous torque, respectively. The five terms in equation 3 constitute the dynamical drivers/terms are the fundamental sources of depth integrated (barotropic) vorticity: on the LHS, the advection of planetary vorticity, on the RHS from left to right, bathymetric interactions through bottom pressure torque, the wind and bottom stress curl, curl of non-linear interactions between terms and the lateral viscous dissipation from within the ocean interior.

The subgrid-scale parameterization introduces a torque, which is included in the viscous torque term. Nonlinear torque is composed of three terms:

$$\nabla \times \mathrm{A} = \nabla \times [\int_{-H}^{\eta} \nabla \cdot (\mathrm{uu}) dz] + [w\zeta]_{z=H}^{z=\eta} + [\nabla w \times \mathrm{u}]_{z=H}^{z=\eta} \tag{A4}$$

where **uu** is a second-order tensor. The right-hand side of equation 4 represents the curl of the vertically integrated momentum flux divergence, the nonlinear contribution to vortex tube stretching, and the conversion of vertical shear to barotropic vorticity. Horizontal viscous forcing includes that induced by subgrid-scale parameterizations. In Sonnewald et al. (2019), twenty-year averaged fields (1992-2013) are used after a Laplacian smoother is applied, with an effective averaging range of three grid cells.

Appendix B Gyre circulation in the subtropical North Atlantic

For the purpose of building intuition, the well-studied subtropical North Atlantic wind gyre will be used to illustrate both the dynamics and the utility found in using objective regime discovery for building hypotheses. The dissipation of vorticity is known to be concentrated along the North American continental boundary (Fig. B1m), while the area of negative wind stress curl is found more centrally in the basin (Fig. B1a). Positive vorticity, needed to balance that input by the wind stress curl is similarly found more centrally in the basin (Fig. B1i), and the vertical transport is weak (Fig. B2a).

In the subtropical North Atlantic (Fig. 1b), the N-SV regime spans the basin after the shelf break from approximately 25-35°N, and extends further north leaning eastwards up to approximately 47°N. At the shelf break to the west, there is a sliver of the NL regime. Note that the streamlines used in previous work are similar to the region covered by the N-SV regime [43]. The SO regime is almost entirely absent. Other dynamical regimes found here are described in [24, 77], and are not needed to support the main points in the present paper.

In the North Atlantic, the SO regime is largely absent for practical purposes and the N-SV and NL regimes will be presented in this section. The wind stress curl is present in the N-SV as a source of predominantly negative vorticity, with the exception of a streak of positive vorticity associated with the mid-Atlantic ridge (Fig. B1b). The NL regime is found along the shelf, where the wind adds both positive and negative vorticity (Fig. B1d). The bottom pressure torque is a largely positive source of vorticity in the N-SV regime, but has notable patches of negative vorticity (Fig. B1f), as with the wind stress curl, the NL regime has a less consistent pattern (Fig. B1h). The advective component has largely positive contribution for the N-SV regime, but the section along the mid-Atlantic ridge is again associated with the opposite contribution (Fig. B1j). The advective component is a source of largely negative vorticity in the NL regime, which is expected from the flow interacting with the shelf and vortex stretching (Fig. B1l). For the non-linear contributions to the vorticity, the N-SV has very little compared to the NL regime, with the main feature being a negative streak along the shelf from the southernmost edge to approximately 32°N (Fig. B1n). For the NL regime the contribution of the non-linear terms is positive (Fig. B1p).

A key distinction between subtropical Northern Hemisphere gyre circulation and that in the Southern Ocean is that the subtropical Northern Hemisphere sees a weak downwelling, while there is a distinct upwelling associated with the Southern Ocean gyre-circulation (also seen in the sub-polar gyre in the North Atlantic).

Appendix C ECCOv4 and the meridional overturning

The overall meridional overturning ($\Psi_{z\theta}$) from Fig. 6 is defined as:

$$\Psi_{z\theta}(\theta, z) = -\int_{-H}^{z} \int_{\phi_2}^{\phi_1} v(\phi, \theta, z') d\phi dz',$$

where z is the relative level depth and v is the meridional (north-south) component of velocity. For the regimes, the relevant velocity fields were then used. A positive $\Psi_{z\theta}$ signifies a clockwise circulation, while a negative $\Psi_{z\theta}$ signifies an anticlockwise circulation.

To assess changes in the global circulation, the meridional overturning streamfuction (Units: 1 Sv=$10^6 m^3/s$) in density space, Ψ_σ [95**?**] is calculated as a function of y (or latitude):

$$\Psi_\sigma(y, t) = \frac{1}{\Delta t} \int_{t}^{t+\Delta t} \int \int_{\sigma' \leq \sigma} v dx dz dt, \tag{C5}$$

where σ is the potential density relative to 2000 dbar, Δt is the timestep (5-days)and v is the meridional velocity.

In decomposing Ψ, we note that Helmholtz' theorem is not valid, and stress that the individual dynamical regime contributions should not be seen as streamfuctions in their own right. This is because large meridional meanders (such as if the ACC were to meanded in and out of a latitudinal range) could imply significant residuals.

Appendix D Additional figures of drivers and resultant currents

Demonstrating the spatial relations of the drivers and the path of the ACC. In Fig. D3 the locations where the ACC reaches the bathymetry and intensifies is demonstrated and its co-location with the NL dynamical regime. This co-location is expected as illustrated in Fig. 8 and 3 where the non-linear torques are associated with the direction of the ACC and the conservation of potential vorticity dictates that the current compresses.

The non-linear torques (Fig. D5) and the bottom pressure torque (Fig. D4) impact the ACC location.

References

[1] Levitus, S., Antonov, J.I., Boyer, T.P., Baranova, O.K., Garcia, H.E., Locarnini, R.A., Mishonov, A.V., Reagan, J.R., Seidov, D., Yarosh, E.S., Zweng, M.M.: World ocean heat content and thermosteric sea level change (0–2000 m), 1955–2010. Geophysical Research Letters **39**(10) (2012)

https://agupubs.onlinelibrary.wiley.com/doi/pdf/10.1029/2012GL051106. https://doi.org/10.1029/2012GL051106

[2] Lenton, T.M., Held, H., Kriegler, E., Hall, J.W., Lucht, W., Rahmstorf, S., Schellnhuber, H.J.: Tipping elements in the earth's climate system. Proceedings of the National Academy of Sciences **105**(6), 1786–1793 (2008) https://www.pnas.org/doi/pdf/10.1073/pnas.0705414105. https://doi.org/10.1073/pnas.0705414105

[3] Paolo, F.S., Fricker, H.A., Padman, L.: Volume loss from antarctic ice shelves is accelerating. Science **348**(6232), 327–331 (2015)

[4] Beadling, R.L., Russell, J.L., Stouffer, R.J., Mazloff, M., Talley, L.D., Goodman, P.J., Sallée, J.B., Hewitt, H.T., Hyder, P., Pandde, A.: Representation of southern ocean properties across coupled model intercomparison project generations: Cmip3 to cmip6. Journal of Climate **33**(15), 6555–6581 (2020). https://doi.org/10.1175/JCLI-D-19-0970.1

[5] Patmore, R.D., Holland, P.R., Munday, D.R., Garabato, A.C.N., Stevens, D.P., Meredith, M.P.: Topographic control of southern ocean gyres and the antarctic circumpolar current: A barotropic perspective. Journal of Physical Oceanography **49**(12), 3221–3244 (2019). https://doi.org/10.1175/JPO-D-19-0083.1

[6] Garabato, A.C.N., Nurser, A.J.G., Scott, R.B., Goff, J.A.: The impact of small-scale topography on the dynamical balance of the ocean. Journal of Physical Oceanography **43**(3), 647–668 (2013). https://doi.org/10.1175/JPO-D-12-056.1

[7] Wilson, E.A., Thompson, A.F., Stewart, A.L., Sun, S.: Bathymetric control of subpolar gyres and the overturning circulation in the southern ocean. Journal of Physical Oceanography **52**(2), 205–223 (2022). https://doi.org/10.1175/JPO-D-21-0136.1

[8] Armitage, T.W.K., Kwok, R., Thompson, A.F., Cunningham, G.: Dynamic topography and sea level anomalies of the southern ocean: Variability and teleconnections. Journal of Geophysical Research: Oceans **123**(1), 613–630 (2018) https://agupubs.onlinelibrary.wiley.com/doi/pdf/10.1002/2017JC013534. https://doi.org/10.1002/2017JC013534

[9] Gille, S.T.: Decadal-scale temperature trends in the southern hemisphere ocean. Journal of Climate **21**(18), 4749–4765 (2008). https://doi.org/10.1175/2008JCLI2131.1

[10] Armour, K., Marshall, J., Scott, J., Donohoe, A., Newsom, E.: Southern ocean warming delayed by circumpolar upwelling and equatorward

transport. Nature Geoscience **9**, 549–554 (2016). https://doi.org/10.1038/ngeo2731

[11] Auger, M., Morrow, R., Kestenare, E., Sallée, J.-b.: Southern ocean in-situ temperature trends over 25 years emerge from interannual variability (2020). https://doi.org/10.21203/rs.3.rs-36449/v1

[12] Marshall, J., Radko, T.: Residual-mean solutions for the antarctic circumpolar current and its associated overturning circulation. Journal of Physical Oceanography - J PHYS OCEANOGR **33** (2003). https://doi.org/10.1175/1520-0485(2003)033⟨2341:RSFTAC⟩2.0.CO;2

[13] Reeve, K.A., Boebel, O., Strass, V., Kanzow, T., Gerdes, R.: Horizontal circulation and volume transports in the weddell gyre derived from argo float data. Progress in Oceanography **175**, 263–283 (2019). https://doi.org/10.1016/j.pocean.2019.04.006

[14] Schröder, M., Fahrbach, E.: On the structure and the transport of the eastern weddell gyre. Deep Sea Research Part II: Topical Studies in Oceanography **46**(1), 501–527 (1999). https://doi.org/10.1016/S0967-0645(98)00112-X

[15] Nadeau, L.-P., Ferrari, R.: The role of closed gyres in setting the zonal transport of the antarctic circumpolar current. Journal of Physical Oceanography **45**(6), 1491–1509 (2015). https://doi.org/10.1175/JPO-D-14-0173.1

[16] Sonnewald, M., Lguensat, R., Jones, D., Düben, P., Brajard, J., Balaji, V.: Bridging observations, theory and numerical simulation of the ocean using machine learning. Environmental Research Letters **16** (2021). https://doi.org/10.1088/1748-9326/ac0eb0

[17] Irrgang, C., Boers, N., Sonnewald, M., Barnes, E., Kadow, C., Staneva, J., Saynisch-Wagner, J.: Will artificial intelligence supersede earth system and climate models? (2021)

[18] Ryan, S., Schröder, M., Huhn, O., Timmermann, R.: On the warm inflow at the eastern boundary of the weddell gyre. Deep Sea Research Part I: Oceanographic Research Papers **107**, 70–81 (2016)

[19] Yamazaki, K., Aoki, S., Shimada, K., Kobayashi, T., Kitade, Y.: Structure of the subpolar gyre in the australian-antarctic basin derived from argo floats. Journal of Geophysical Research: Oceans **125**(8), 2019–015406 (2020) https://agupubs.onlinelibrary.wiley.com/doi/pdf/10.1029/2019JC015406. https://doi.org/10.1029/2019JC015406. e2019JC015406 2019JC015406

[20] Yamazaki, K., Aoki, S., Katsumata, K., Hirano, D., Nakayama, Y.: Multidecadal poleward shift of the southern boundary of the Antarctic Circumpolar Current off East Antarctica. Science Advances **7**(24), 8755 (2021). https://doi.org/10.1126/sciadv.abf8755

[21] Meijers, A.J.S., Klocker, A., Bindoff, N.L., Williams, G.D., Marsland, S.J.: The circulation and water masses of the antarctic shelf and continental slope between 30 and 80e. Deep Sea Research Part II: Topical Studies in Oceanography **57**(9), 723–737 (2010). https://doi.org/10.1016/j.dsr2.2009.04.019. "BROKE-West" a Biological/Oceanographic Survey Off the Coast of East Antarctica (30-80°E) Carried Out in January-March 2006

[22] McCartney, M.S., Donohue, K.A.: A deep cyclonic gyre in the australian–antarctic basin. Progress in Oceanography **75**(4), 675–750 (2007). https://doi.org/10.1016/j.pocean.2007.02.008

[23] Bindoff, N.L., Rosenberg, M.A., Warner, M.J.: On the circulation and water masses over the antarctic continental slope and rise between 80 and 150 e. Deep Sea Research Part II: Topical Studies in Oceanography **47**(12-13), 2299–2326 (2000)

[24] Sonnewald, M., Wunsch, C., Heimbach, P.: Unsupervised learning reveals geography of global ocean dynamical regions. Earth and Space Science **6**(5), 784–794 (2019) https://agupubs.onlinelibrary.wiley.com/doi/pdf/10.1029/2018EA000519. https://doi.org/10.1029/2018EA000519

[25] Kaiser, B.E., Saenz, J.A., Sonnewald, M., Livescu, D.: Automated identification of dominant physical processes. Engineering Applications of Artificial Intelligence **116**, 105496 (2022). https://doi.org/10.1016/j.engappai.2022.105496

[26] Sverdrup, H.U.: Wind-driven currents in a baroclinic ocean; with application to the equatorial currents of the eastern pacific. Proceedings of the National Academy of Sciences **33**(11), 318–326 (1947) https://www.pnas.org/content/33/11/318.full.pdf. https://doi.org/10.1073/pnas.33.11.318

[27] Munk, W.H.: ON THE WIND-DRIVEN OCEAN CIRCULATION. Journal of Meteorology **7**(2), 80–93 (1950) https://journals.ametsoc.org/jas/article-pdf/7/2/80/3692186/1520-0469(1950)007_0080_otwdoc_2_0_co_2.pdf. https://doi.org/10.1175/1520-0469(1950)007⟨0080:OTWDOC⟩2.0.CO;2

[28] Stommel, H.: The westward intensification of wind-driven ocean currents. Transactions, American Geophysical Union **29**(2), 202–206 (1948). https://doi.org/10.1029/TR029i002p00202

[29] Hughes, C.W., de Cuevas, B.A.: Why Western Boundary Currents in Realistic Oceans are Inviscid: A Link between Form Stress and Bottom Pressure Torques. Journal of Physical Oceanography **31**(10), 2871–2885 (2001) https://journals.ametsoc.org/jpo/article-pdf/31/10/2871/4450500/1520-0485(2001)031_2871_wwbcir_2_0_co_2.pdf. https://doi.org/10.1175/1520-0485(2001)031⟨2871:WWBCIR⟩2.0.CO;2

[30] Hughes, C.W., de Cuevas, B.A.: Why western boundary currents in realistic oceans are inviscid: A link between form stress and bottom pressure torques. Journal of Physical Oceanography **31**(10), 2871–2885 (2001). https://doi.org/10.1175/1520-0485(2001)031⟨2871:WWBCIR⟩2.0.CO;2

[31] Munk, W.H.: ON THE WIND-DRIVEN OCEAN CIRCULATION. Journal of Meteorology **7**(2), 80–93 (1950) https://journals.ametsoc.org/jas/article-pdf/7/2/80/3692186/1520-0469(1950)007_0080_otwdoc_2_0_co_2.pdf. https://doi.org/10.1175/1520-0469(1950)007⟨0080:OTWDOC⟩2.0.CO;2

[32] Holland, W.R.: Baroclinic and topographic influences on the transport in western boundary currents. Geophysical and Astrophysical Fluid Dynamics **4**(1), 187–210 (1972). https://doi.org/10.1080/03091927208236095

[33] Schoonover, J., Dewar, W., Wienders, N., Gula, J., McWilliams, J.C., Molemaker, M.J., Bates, S.C., Danabasoglu, G., Yeager, S.: North Atlantic Barotropic Vorticity Balances in Numerical Models*. Journal of Physical Oceanography **46**(1), 289–303 (2016) https://journals.ametsoc.org/jpo/article-pdf/46/1/289/4579669/jpo-d-15-0133_1.pdf. https://doi.org/10.1175/JPO-D-15-0133.1

[34] Yeager, S.: Topographic Coupling of the Atlantic Overturning and Gyre Circulations. Journal of Physical Oceanography **45**(5), 1258–1284 (2015) https://journals.ametsoc.org/jpo/article-pdf/45/5/1258/4559431/jpo-d-14-0100_1.pdf. https://doi.org/10.1175/JPO-D-14-0100.1

[35] Jackson, L., Hughes, C.W., Williams, R.G.: Topographic control of basin and channel flows: The role of bottom pressure torques and friction. Journal of Physical Oceanography **36**(9), 1786–1805 (2006). https://doi.org/10.1175/JPO2936.1

[36] Le Bras, I.A.-A., Sonnewald, M., Toole, J.M.: A Barotropic Vorticity Budget for the Subtropical North Atlantic Based on Observations. Journal of Physical Oceanography **49**(11), 2781–2797 (2019) https://journals.ametsoc.org/jpo/article-pdf/49/11/2781/4853904/jpo-d-19-0111_1.pdf. https://doi.org/10.1175/JPO-D-19-0111.1

[37] Thomas, M.D., Boer, A.M.D., Johnson, H.L., Stevens, D.P.: Spatial and

temporal scales of sverdrup balance. Journal of Physical Oceanography **44**(10), 2644–2660 (2014). https://doi.org/10.1175/JPO-D-13-0192.1

[38] Stommel, H.: The westward intensification of wind-driven ocean currents. Eos, Transactions American Geophysical Union **29**(2), 202–206 (1948) https://agupubs.onlinelibrary.wiley.com/doi/pdf/10.1029/TR029i002p00202. https://doi.org/10.1029/TR029i002p00202

[39] Sverdrup, H.U.: Wind-driven currents in a baroclinic ocean; with application to the equatorial currents of the eastern pacific*. Proceedings of the National Academy of Sciences **33**(11), 318–326 (1947) https://www.pnas.org/doi/pdf/10.1073/pnas.33.11.318. https://doi.org/10.1073/pnas.33.11.318

[40] Rhines, P.B.: Vorticity dynamics of the oceanic general circulation. Annual Review of Fluid Mechanics **18**(1), 433–497 (1986) https://doi.org/10.1146/annurev.fl.18.010186.002245. https://doi.org/10.1146/annurev.fl.18.010186.002245

[41] Luyten, J., Stommel, H.: Gyres driven by combined wind and buoyancy flux. Journal of Physical Oceanography **16**(9), 1551–1560 (1986). https://doi.org/10.1175/1520-0485(1986)016⟨1551:GDBCWA⟩2.0.CO;2

[42] Stewart, A.L., McWilliams, J.C., Solodoch, A.: On the role of bottom pressure torques in wind-driven gyres. Journal of Physical Oceanography **51**(5), 1441–1464 (2021). https://doi.org/10.1175/JPO-D-20-0147.1

[43] Schoonover, J., Dewar, W., Wienders, N., Gula, J., McWilliams, J., Molemaker, M., Bates, S., Danabasoglu, G., Yeager, S.: North atlantic barotropic vorticity balances in numerical models. Journal of Physical Oceanography **46** (2016). https://doi.org/10.1175/JPO-D-15-0133.1

[44] Le Corre, M., Gula, J., Tréguier, A.-M.: Barotropic vorticity balance of the north atlantic subpolar gyre in an eddy-resolving model. Ocean Science **16**(2), 451–468 (2020). https://doi.org/10.5194/os-16-451-2020

[45] Speich, S., Blanke, B., Cai, W.: Atlantic meridional overturning circulation and the southern hemisphere supergyre. Geophysical Research Letters **34**(23) (2007) https://agupubs.onlinelibrary.wiley.com/doi/pdf/10.1029/2007GL031583. https://doi.org/10.1029/2007GL031583

[46] Ridgway, K.R., Dunn, J.R.: Observational evidence for a southern hemisphere oceanic supergyre. Geophysical Research Letters **34**(13) (2007) https://agupubs.onlinelibrary.wiley.com/doi/pdf/10.1029/2007GL030392. https://doi.org/10.1029/2007GL030392

[47] Qu, T., Fukumori, I., Fine, R.A.: Spin-up of the southern hemisphere super gyre. Journal of Geophysical Research: Oceans **124**(1), 154–170 (2019) https://agupubs.onlinelibrary.wiley.com/doi/pdf/10.1029/2018JC014391. https://doi.org/10.1029/2018JC014391

[48] Chapman, C., Lea, M.-A., Meyer, A., Sallée, J.-b., Hindell, M.: Defining southern ocean fronts and their influence on biological and physical processes in a changing climate. Nature Climate Change **10**, 1–11 (2020). https://doi.org/10.1038/s41558-020-0705-4

[49] Huang, X., Stärz, M., Gohl, K., Knorr, G., Lohmann, G.: Impact of weddell sea shelf progradation on antarctic bottom water formation during the miocene. Paleoceanography **32**(3), 304–317 (2017) https://agupubs.onlinelibrary.wiley.com/doi/pdf/10.1002/2016PA002987. https://doi.org/10.1002/2016PA002987

[50] Park, Y.-H., Gambéroni, L.: Large-scale circulation and its variability in the south indian ocean from topex/poseidon altimetry. Journal of Geophysical Research: Oceans **100**(C12), 24911–24929 (1995) https://agupubs.onlinelibrary.wiley.com/doi/pdf/10.1029/95JC01962. https://doi.org/10.1029/95JC01962

[51] Dotto, T.S., Naveira Garabato, A., Bacon, S., Tsamados, M., Holland, P.R., Hooley, J., Frajka-Williams, E., Ridout, A., Meredith, M.P.: Variability of the ross gyre, southern ocean: Drivers and responses revealed by satellite altimetry. Geophysical Research Letters **45**(12), 6195–6204 (2018) https://agupubs.onlinelibrary.wiley.com/doi/pdf/10.1029/2018GL078607. https://doi.org/10.1029/2018GL078607

[52] Meredith, M.P., Jullion, L., Brown, P.J., Naveira Garabato, A.C., Couldrey, M.P.: Dense waters of the weddell and scotia seas: recent changes in properties and circulation. Philosophical Transactions of the Royal Society A: Mathematical, Physical and Engineering Sciences **372**(2019), 20130041 (2014) https://royalsocietypublishing.org/doi/pdf/10.1098/rsta.2013.0041. https://doi.org/10.1098/rsta.2013.0041

[53] Brown, P.J., Jullion, L., Landschützer, P., Bakker, D.C.E., Naveira Garabato, A.C., Meredith, M.P., Torres-Valdés, S., Watson, A.J., Hoppema, M., Loose, B., Jones, E.M., Telszewski, M., Jones, S.D., Wanninkhof, R.: Carbon dynamics of the weddell gyre, southern ocean. Global Biogeochemical Cycles **29**(3), 288–306 (2015) https://agupubs.onlinelibrary.wiley.com/doi/pdf/10.1002/2014GB005006. https://doi.org/10.1002/2014GB005006

[54] Heywood, K., Sparrow, M., Brown, J., Dickson, R.: Frontal structure and antarctic bottom water flow through the princess elizabeth trough, antarctica. Deep Sea Research Part I: Oceanographic Research Papers **46**(7), 1181–1200 (1999). https://doi.org/10.1016/S0967-0637(98)00108-3

[55] Meijers, A.J.S., Shuckburgh, E., Bruneau, N., Sallee, J.-B., Bracegirdle, T.J., Wang, Z.: Representation of the antarctic circumpolar current in the cmip5 climate models and future changes under warming scenarios. Journal of Geophysical Research: Oceans **117**(C12) (2012) https://agupubs.onlinelibrary.wiley.com/doi/pdf/10.1029/2012JC008412. https://doi.org/10.1029/2012JC008412

[56] Vernet, M., Geibert, W., Hoppema, M., Brown, P.J., Haas, C., Hellmer, H.H., Jokat, W., Jullion, L., Mazloff, M., Bakker, D.C.E., Brearley, J.A., Croot, P., Hattermann, T., Hauck, J., Hillenbrand, C.-D., Hoppe, C.J.M., Huhn, O., Koch, B.P., Lechtenfeld, O.J., Meredith, M.P., Naveira Garabato, A.C., Nöthig, E.-M., Peeken, I., Rutgers van der Loeff, M.M., Schmidtko, S., Schröder, M., Strass, V.H., Torres-Valdés, S., Verdy, A.: The weddell gyre, southern ocean: Present knowledge and future challenges. Reviews of Geophysics **57**(3), 623–708 (2019) https://agupubs.onlinelibrary.wiley.com/doi/pdf/10.1029/2018RG000604. https://doi.org/10.1029/2018RG000604

[57] Deacon, G.E.R.: The weddell gyre. Deep Sea Research Part A. Oceanographic Research Papers **26**(9), 981–995 (1979). https://doi.org/10.1016/0198-0149(79)90044-X

[58] Mackintosh, N.A.: Life cycle of antarctic krill in relation to ice and water conditions. Discovery Rep. **36**, 1–94 (1972)

[59] Park, Y.-H., Charriaud, E., Craneguy, P., Kartavtseff, A.: Fronts, transport, and weddell gyre at 30 e between africa and antarctica. Journal of Geophysical Research: Oceans **106**(C2), 2857–2879 (2001)

[60] Fahrbach, E., Hoppema, M., Rohardt, G., Schröder, M., Wisotzki, A.: Decadal-scale variations of water mass properties in the deep weddell sea. Ocean Dynamics **54**, 77–91 (2004). https://doi.org/10.1007/s10236-003-0082-3

[61] Fahrbach, E., Hoppema, M., Rohardt, G., Boebel, O., Klatt, O., Wisotzki, A.: Warming of deep and abyssal water masses along the greenwich meridian on decadal time scales: The weddell gyre as a heat buffer. Deep Sea Research Part II: Topical Studies in Oceanography **58**(25-26), 2509–2523 (2011)

[62] Strass, V.H., Rohardt, G., Kanzow, T., Hoppema, M., Boebel, O.: Multidecadal warming and density loss in the deep weddell sea, antarctica.

Journal of Climate **33**(22), 9863–9881 (2020). https://doi.org/10.1175/JCLI-D-20-0271.1

[63] Gouretski, V.: The Large-Scale Thermohaline Structure of the Ross Gyre, pp. 77–100 (1999). https://doi.org/10.1007/978-88-470-2250-8_6

[64] Jacobs, S.S., Giulivi, C.F., Mele, P.A.: Freshening of the ross sea during the late 20th century. Science **297**(5580), 386–389 (2002) https://www.science.org/doi/pdf/10.1126/science.1069574. https://doi.org/10.1126/science.1069574

[65] Park, Y.-H., Gambéroni, L.: Large-scale circulation and its variability in the south indian ocean from topex/poseidon altimetry. Journal of Geophysical Research: Oceans **100**(C12), 24911–24929 (1995) https://agupubs.onlinelibrary.wiley.com/doi/pdf/10.1029/95JC01962. https://doi.org/10.1029/95JC01962

[66] Nakayama, Y., Timmermann, R., Schröder, M., Hellmer, H.H.: On the difficulty of modeling circumpolar deep water intrusions onto the amundsen sea continental shelf. Ocean Modelling **84**, 26–34 (2014). https://doi.org/10.1016/j.ocemod.2014.09.007

[67] Gnanadesikan, A.: A simple predictive model for the structure of the oceanic pycnocline. Science **283**(5410), 2077–2079 (1999) https://www.science.org/doi/pdf/10.1126/science.283.5410.2077. https://doi.org/10.1126/science.283.5410.2077

[68] Nikurashin, M., Vallis, G.: A theory of the interhemispheric meridional overturning circulation and associated stratification. Journal of Physical Oceanography **42**(10), 1652–1667 (2012). https://doi.org/10.1175/JPO-D-11-0189.1

[69] Thompson, A.F., Stewart, A.L., Bischoff, T.: A multibasin residual-mean model for the global overturning circulation. Journal of Physical Oceanography **46**(9), 2583–2604 (2016). https://doi.org/10.1175/JPO-D-15-0204.1

[70] Youngs, M.K., Flierl, G.R., Ferrari, R.: Role of residual overturning for the sensitivity of southern ocean isopycnal slopes to changes in wind forcing. Journal of Physical Oceanography **49**(11), 2867–2881 (2019). https://doi.org/10.1175/JPO-D-19-0072.1

[71] Döös, K.: Interocean exchange of water masses. Journal of Geophysical Research: Oceans **100**(C7), 13499–13514 (1995)

[72] Tamsitt, V., Drake, H., Morrison, A., Talley, L., Dufour, C., Gray,

A., Griffies, S., Mazloff, M., Sarmiento, J., Wang, J., Weijer, W.: Spiraling pathways of global deep waters to the surface of the southern ocean. Nature Communications **8**, 172 (2017). https://doi.org/10.1038/s41467-017-00197-0

[73] Viglione, G.A., Thompson, A.F.: Lagrangian pathways of upwelling in the southern ocean. Journal of Geophysical Research: Oceans **121**(8), 6295–6309 (2016) https://agupubs.onlinelibrary.wiley.com/doi/pdf/10.1002/2016JC011773. https://doi.org/10.1002/2016JC011773

[74] IPCC21: In: V. Masson-Delmotte, A.P.S.L.C.C.P.S.B.N.C.Y.C.L.G.M.I.G.M.H.K.L.E P. Zhai, Zhou, B. (eds.) Summary for Policymakers. Cambridge University Press, Cambridge, United Kingdom and New York, NY, USA (2021). https://doi.org/10.1017/9781009157896. www.climatechange2021.org

[75] Meredith, M.P., Garabato, A.C.N., Hogg, A.M., Farneti, R.: Sensitivity of the overturning circulation in the southern ocean to decadal changes in wind forcing. Journal of Climate **25**(1), 99–110 (2012). https://doi.org/10.1175/2011JCLI4204.1

[76] Morrison, A.K., Hogg, A.M.: On the relationship between southern ocean overturning and acc transport. Journal of Physical Oceanography **43**(1), 140–148 (2013). https://doi.org/10.1175/JPO-D-12-057.1

[77] Sonnewald, M., Lguensat, R.: Revealing the impact of global heating on north atlantic circulation using transparent machine learning. Journal of Advances in Modeling Earth Systems **13**(8), 2021–002496 (2021) https://agupubs.onlinelibrary.wiley.com/doi/pdf/10.1029/2021MS002496. https://doi.org/10.1029/2021MS002496. e2021MS002496 2021MS002496

[78] Forget, G., Campin, J.-M., Heimbach, P., Hill, C., Ponte, R., Wunsch, C.: Ecco version 4: An integrated framework for non-linear inverse modeling and global ocean state estimation. Geoscientific Model Development Discussions **8**, 3653–3743 (2015). https://doi.org/10.5194/gmdd-8-3653-2015

[79] Wunsch, C., Heimbach, P.: Chapter 21 - dynamically and kinematically consistent global ocean circulation and ice state estimates. In: Siedler, G., Griffies, S.M., Gould, J., Church, J.A. (eds.) Ocean Circulation and Climate. International Geophysics, vol. 103, pp. 553–579. Academic Press, ??? (2013). https://doi.org/10.1016/B978-0-12-391851-2.00021-0. http://www.sciencedirect.com/science/article/pii/B9780123918512000210

[80] Adcroft, A., Hill, C., Campin, J.-M., Marshall, J., Heimbach, P.: Overview of the formulation and numerics of the mit gcm. In: Proceedings of the ECMWF Seminar Series on Numerical Methods, Recent Developments in

Numerical Methods for Atmosphere and Ocean Modelling, pp. 139–149 (2004)

[81] Smith, N.R., Zhaoqian, D., Kerry, K.R., Wright, S.: Water masses and circulation in the region of prydz bay, antarctica. Deep Sea Research Part A. Oceanographic Research Papers **31**(9), 1121–1147 (1984). https://doi.org/10.1016/0198-0149(84)90016-5

[82] Aoki, S., Sasai, Y., Sasaki, H., Mitsudera, H., Williams, G.: The cyclonic circulation in the australian–antarctic basin simulated by an eddy-resolving general circulation model. Ocean Dynamics **60**, 743–757 (2010). https://doi.org/10.1007/s10236-009-0261-y

[83] Pardo, P.C., Pérez, F.F., Velo, A., Gilcoto, M.: Water masses distribution in the southern ocean: Improvement of an extended omp (eomp) analysis. Progress in Oceanography **103**, 92–105 (2012). https://doi.org/10.1016/j.pocean.2012.06.002

[84] Dufour, C.O., Griffies, S.M., de Souza, G.F., Frenger, I., Morrison, A.K., Palter, J.B., Sarmiento, J.L., Galbraith, E.D., Dunne, J.P., Anderson, W.G., Slater, R.D.: Role of mesoscale eddies in cross-frontal transport of heat and biogeochemical tracers in the southern ocean. Journal of Physical Oceanography **45**(12), 3057–3081 (2015). https://doi.org/10.1175/JPO-D-14-0240.1

[85] Brady, R.X., Maltrud, M.E., Wolfram, P.J., Drake, H.F., Lovenduski, N.S.: The influence of ocean topography on the upwelling of carbon in the southern ocean. Geophysical Research Letters **48**(19), 2021–095088 (2021) https://agupubs.onlinelibrary.wiley.com/doi/pdf/10.1029/2021GL095088. https://doi.org/10.1029/2021GL095088. e2021GL095088 2021GL095088

[86] Forget, G., Ferreira, D., Liang, X.: On the observability of turbulent transport rates by argo: supporting evidence from an inversion experiment. Ocean Science **11**(5), 839–853 (2015). https://doi.org/10.5194/os-11-839-2015

[87] Cisewski, B., Strass, V.H., Leach, H.: Circulation and transport of water masses in the lazarev sea, antarctica, during summer and winter 2006. Deep Sea Research Part I: Oceanographic Research Papers **58**(2), 186–199 (2011)

[88] Núñez-Riboni, I., Fahrbach, E.: Seasonal variability of the antarctic coastal current and its driving mechanisms in the weddell sea. Deep Sea Research Part I: Oceanographic Research Papers **56**(11), 1927–1941 (2009)

[89] Wang, G., Cai, W., Santoso, A., Wu, L., Fyfe, J., Yeh, S.-W., Ng, B., Yang,

K., McPhaden, M.: Future southern ocean warming linked to projected enso variability. Nature Climate Change **12**, 1–6 (2022). https://doi.org/10.1038/s41558-022-01398-2

[90] Viebahn, J.P., von der Heydt, A.S., Le Bars, D., Dijkstra, H.A.: Effects of drake passage on a strongly eddying global ocean. Paleoceanography **31**(5), 564–581 (2016) https://agupubs.onlinelibrary.wiley.com/doi/pdf/10.1002/2015PA002888. https://doi.org/10.1002/2015PA002888

[91] Sauermilch, I., Whittaker, J., Klocker, A., Munday, D., Hochmuth, K., Bijl, P., Lacasce, J.: Gateway-driven weakening of ocean gyres leads to southern ocean cooling. Nature Communications **12**, 6465 (2021). https://doi.org/10.1038/s41467-021-26658-1

[92] Scher, H., Whittaker, J., Williams, S., Latimer, J., Kordesch, W., Delaney, M.: Onset of antarctic circumpolar current 30 million years ago as tasmanian gateway aligned with westerlies. Nature **523**, 2015 (2015). https://doi.org/10.1038/nature14598

[93] Bijl, P.K., Houben, A.J.P., Hartman, J.D., Pross, J., Salabarnada, A., Escutia, C., Sangiorgi, F.: Paleoceanography and ice sheet variability offshore wilkes land, antarctica – part 2: Insights from oligocene–miocene dinoflagellate cyst assemblages. Climate of the Past **14**(7), 1015–1033 (2018). https://doi.org/10.5194/cp-14-1015-2018

[94] Huber, M., Brinkhuis, H., Stickley, C.E., Döös, K., Sluijs, A., Warnaar, J., Schellenberg, S.A., Williams, G.L.: Eocene circulation of the southern ocean: Was antarctica kept warm by subtropical waters? Paleoceanography **19**(4) (2004) https://agupubs.onlinelibrary.wiley.com/doi/pdf/10.1029/2004PA001014. https://doi.org/10.1029/2004PA001014

[95] Zika, J.D., England, M.H., Sijp, W.P.: The Ocean Circulation in Thermohaline Coordinates. Journal of Physical Oceanography **42**(5), 708–724 (2012) https://journals.ametsoc.org/jpo/article-pdf/42/5/708/4524931/jpo-d-11-0139_1.pdf. https://doi.org/10.1175/JPO-D-11-0139.1

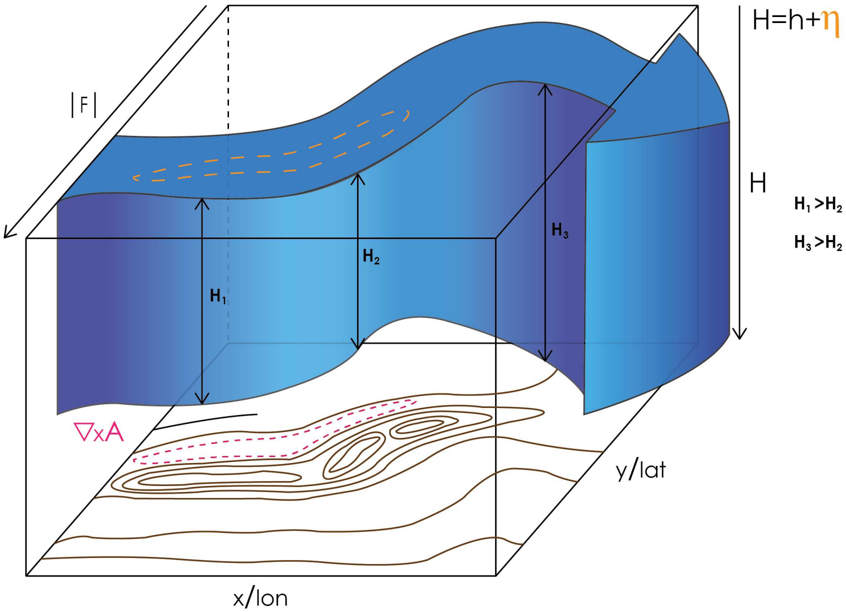

Fig. 3 Illustration of topographic interactions, non-linear torque and dynamic sea level. The pink colour illustrates where one could expect the non-linear torques to be found relative to a bathymetric obstacle illustrated with the brown contours. The large arrow is a representation of a strong zonal current, with the depth being changed relative to the obstacle. The sea surface change is proportional to the pressure buildup and offset from the bathymetric obstacle. Figure not to scale and intended for strictly illustration purposes.

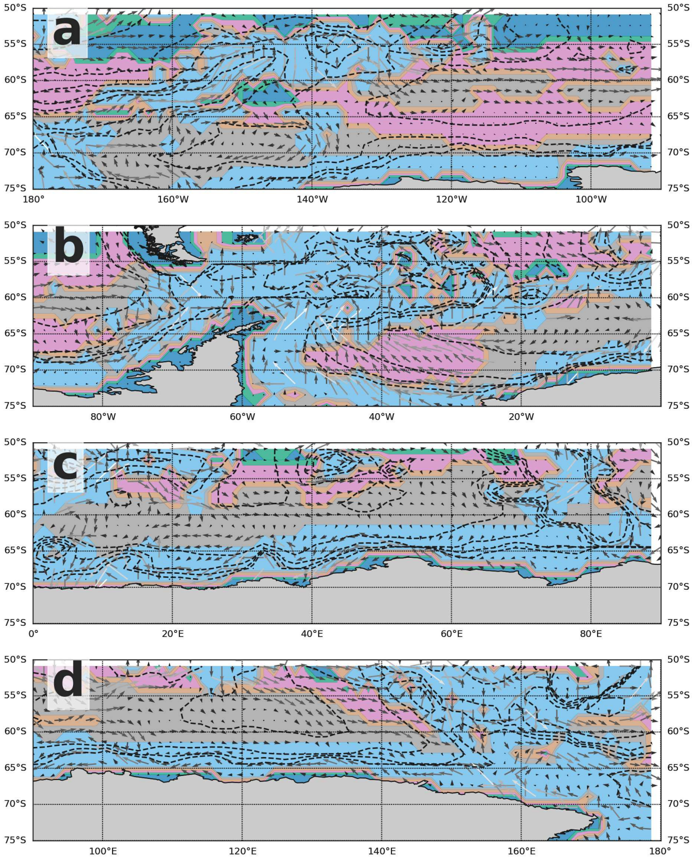

Fig. 4 Current direction in bottom layers. The current magnitudes of the bottom five grid cells. The arrows are scaled to illustrate the relative magnitudes. The velocities are very different, and for clarity the arrows are also shaded in grey-scale where large magnitudes are in white and less intense currents are in white. The path of the Antarctic Circumpolar Current is illustrated further in Fig. D3. The colours are the dynamical regimes, where the grey is the SO topographic Sverdrup regime, the pink in the N-SV Sverdrupian regime, and the light blue is the NL regime where non-linear terms dominate. Stippled lines are the geostrophic contours.

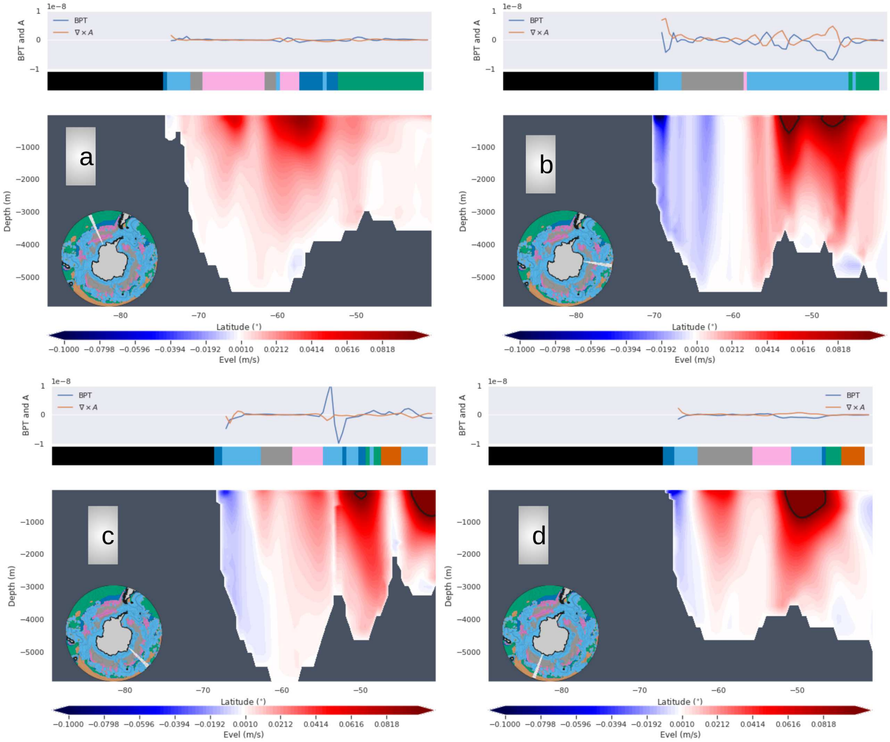

Fig. 5 Transect. Composite figures of different transects. Within each figure: Top shows the bottom pressure torque and $\nabla \times A$, the middle shows the present dynamical regimes and the lower shows the zonal velocities with eastwards being positive. The black contour. The inset global illustrates the location of the transect with a white line, and colours on the globe are the dynamical regimes as shown in Fig. 1a.

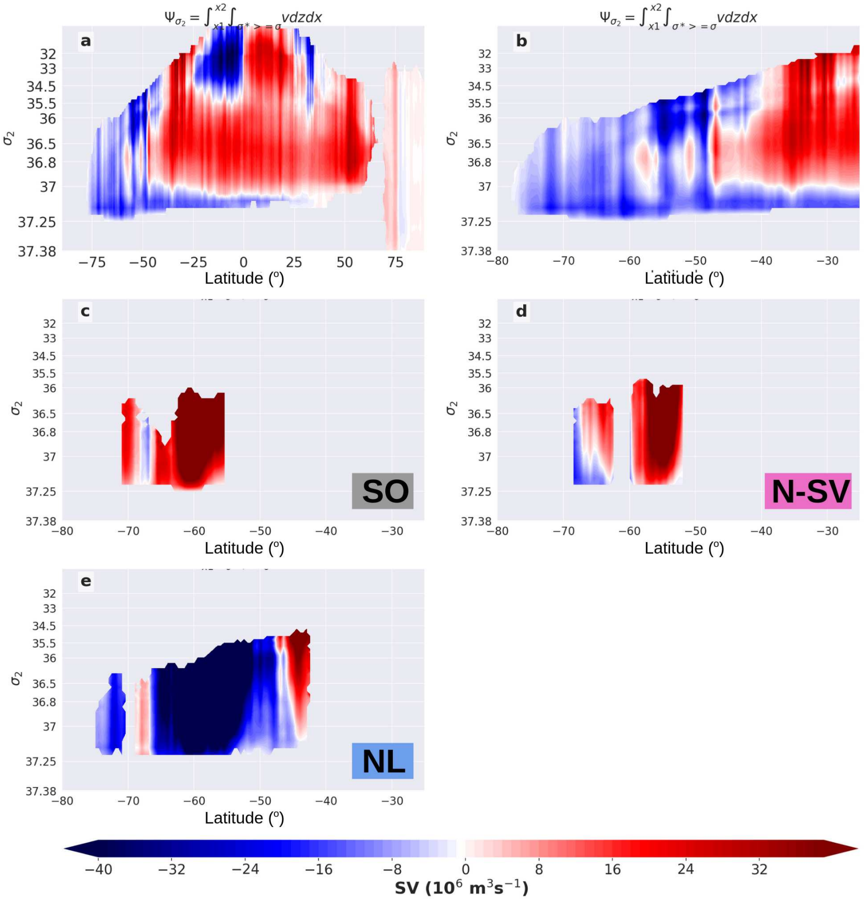

Fig. 6 The streamfunction (Ψ) in density coordinates (σ_2), and the contribution of individual dynamical regimes. The full streamfunction is shown in panel a, and panel b shows a closeup of the Southern Ocean region. Panel c shows the component of the streamfuction given by using only the meridional circulation present in the topographic Sverdrup balance (SO, grey) regime, panel d shows the Sverdrupian (N-SV, pink) regime and panel e shows the non-linear regime (NL, light blue). Adding panels c, d and e would result in the full streamfunction depicted in panels a and b. Red denotes clockwise and blue denotes counterclockwise circulation.

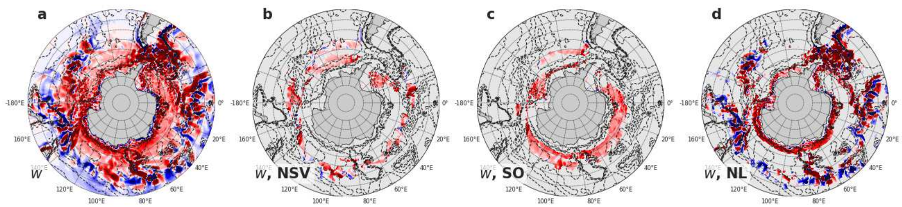

Fig. 7 The vertical velocity (w, $m^s s^{-1}$). The w broken down by dynamical regime, integrated from ca. 550 to 4000m. Panel a shows the full region, panel b the N-SV regime, panel c the SO regime and panel d the NL regime.

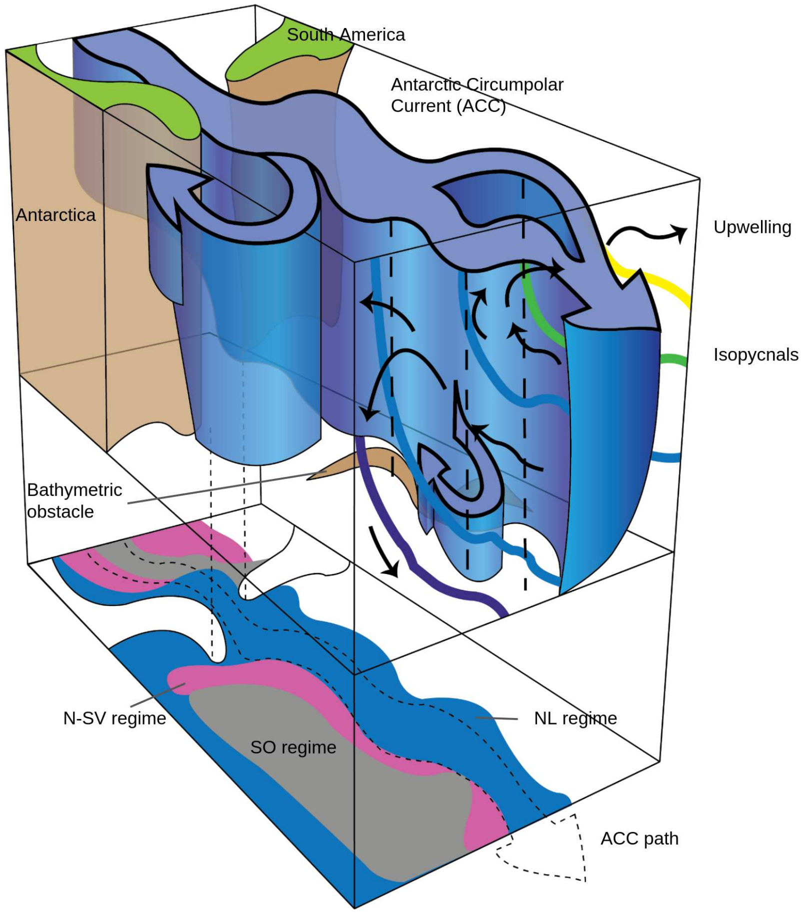

Fig. 8 Sketch of overall dynamics. The Antarctic Circumpolar Current (ACC, large blue arrow and stippled line on bottom) squeezes through the Drake Passage between Antarctica and South America. Dissipation, revealed as nonlinearities in the NL regime (light blue) are heightened where the ACC veers North encountering bathymetry (brown), and elevated dissipation allows a clockwise circulation following the obstacle. In the SO regime (gray) upwelling is seen as a result, as isopycnals (coloured lines showing overall effect in whole box with purple to yellow indicating decreasing density) tilt upwards as a result of strong winds southwards of the ACC.

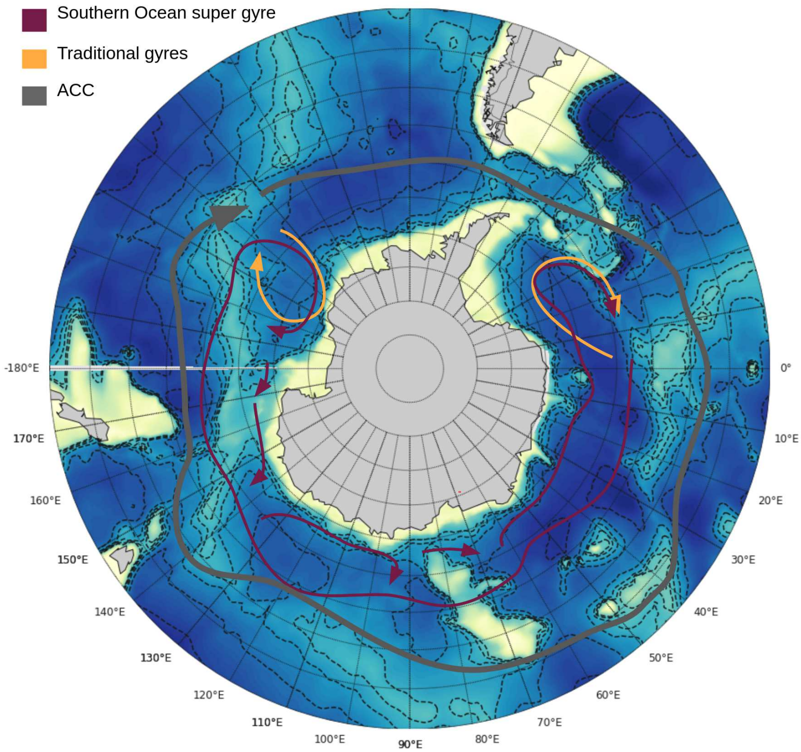

Fig. 9 Sketch illustrating difference in old and proposed frameworks. The yellow arrows indicate where the individual gyres are located, in the Weddell and Ross gyres. The magenta arrows indicate the area covered by the supergyre. The gray arow is a very rough approximate location of the ACC represented as just one arrow.

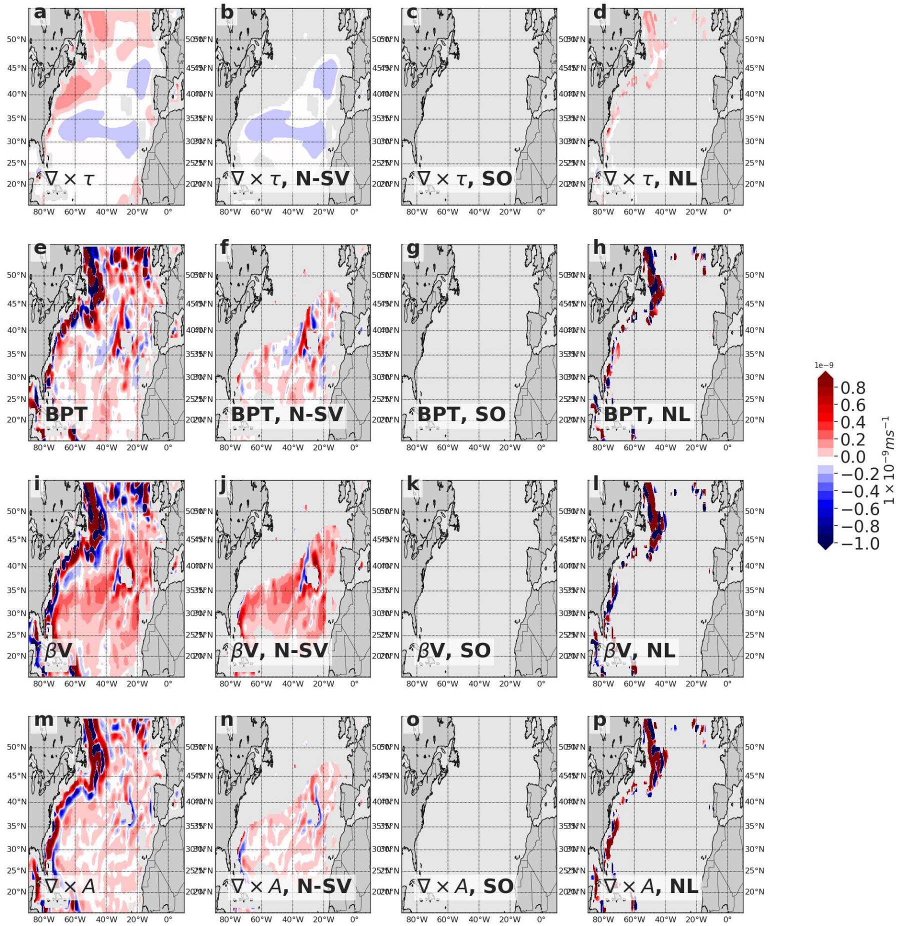

Fig. B1 The terms of the barotropic vorticity equation centered on the subtropical North Atlantic. The first row (a-d) represent the wind stress curn ($\nabla \times \tau$). The second row from the top show the bottom pressure torque (e-h, BPT). The third row from the top represents the advective component of the flow (i-l, $\beta \mathbf{V}$). The bottom row represents the curl of the non-linear terms (m-p, $\nabla \times \mathbf{A}$). The portions in columns two to four anr broken down by dynamical regime. The first column a shows the full region, column two the N-SV regime, column three the SO regime and column four the NL regime.

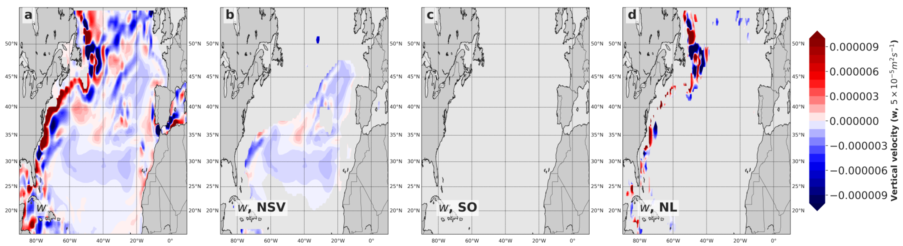

Fig. B2 The vertical velocity (w, $m^s s^{-1}$). The w broken down by dynamical regime, integrated from ca. 550 to 4000m. Panel a shows the full region, panel b the N-SV regime, panel c the SO regime and panel d the NL regime.

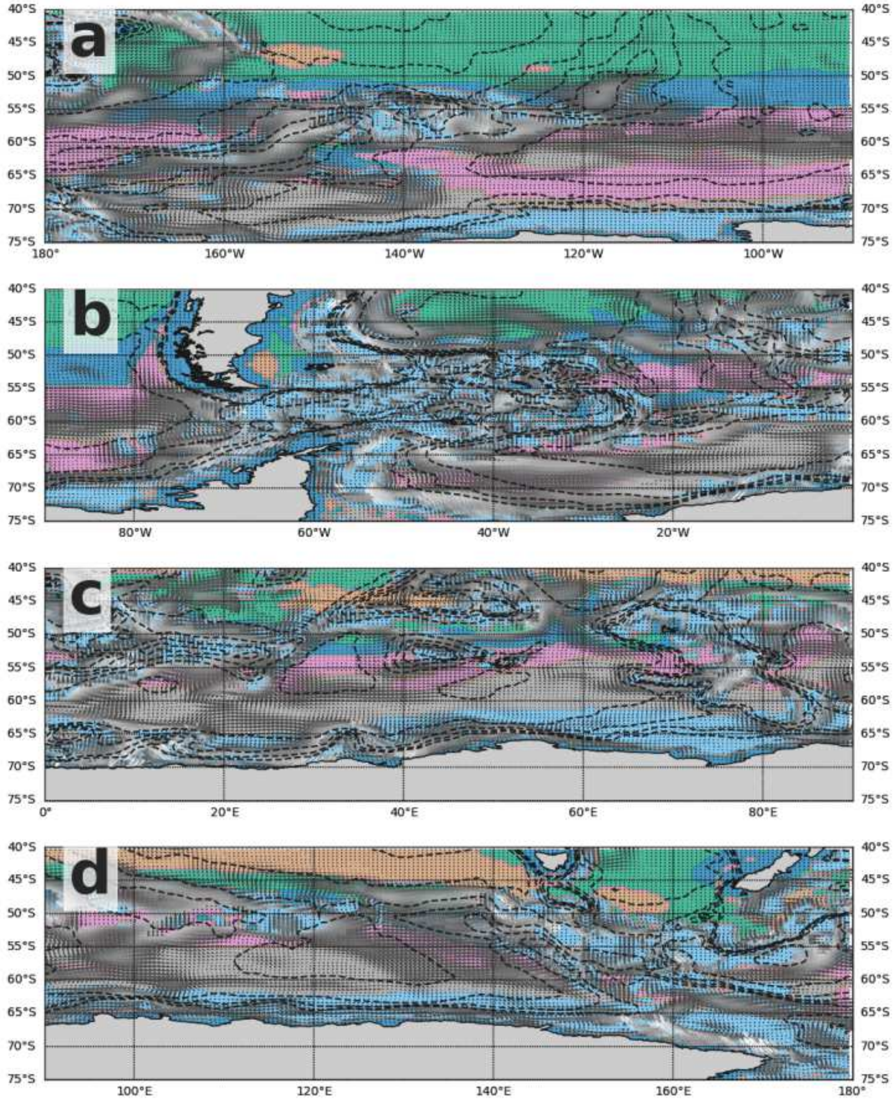

Fig. D3 Flow scaled to illustrate intense currents. The current magnitudes of the bottom five grid cells. Arrows are scaled slightly and coloured as in Fig. 4. Colours represent the dynamical regimes. The black lines are contours of H. Note the regions of current intensification associated with bathymetric obstacles and areas where several jets form.

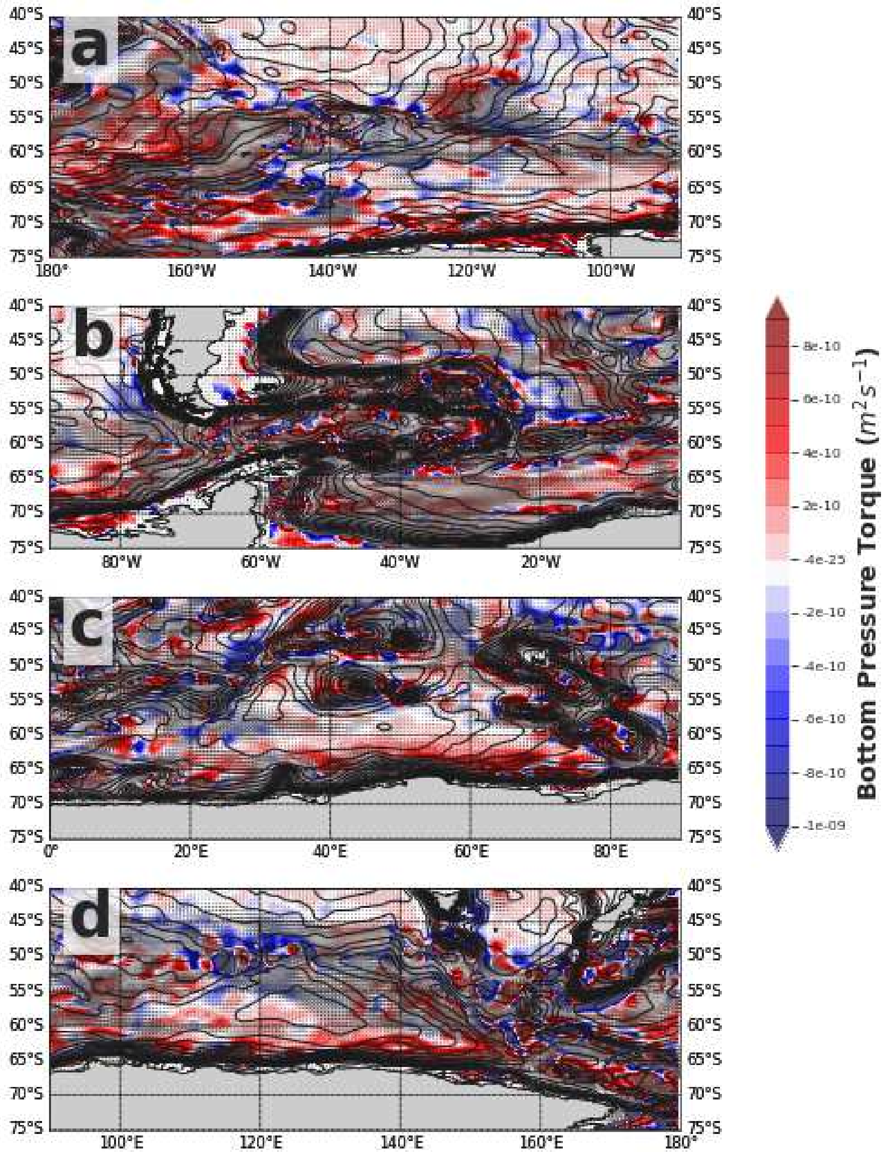

Fig. D4 The bottom pressure torque and flow. Colours represent the bottom pressure torque, arrows are gray-scaled and their magnitude scaled to reveal structures. The black lines are contours of H.

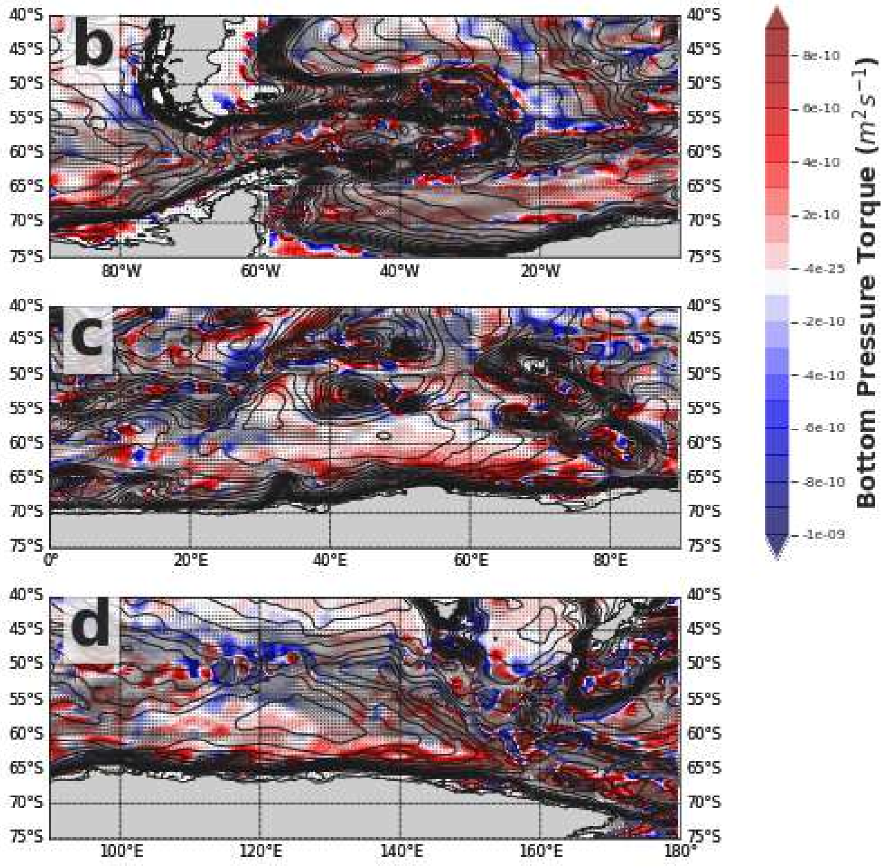

Fig. D5 The non-linear torques and flow. Colours represent the non-linear torques, arrows are gray-scaled and their magnitude scaled to reveal structures. The black lines are contours of H.